NASA Contractor Report 180861

NASA-CR-180861
19880018690

Structural Tailoring of Advanced Turboprops (STAT)

Interim Report

K. Brown
UNITED TECHNOLOGIES CORPORATION
Pratt & Whitney
400 Main Street
East Hartford, CT 06108

August 1988

Prepared for
Lewis Research Center
Under Contract NAS3-23941

National Aeronautics and
Space Administration

UNITED TECHNOLOGIES
PRATT&WHITNEY

400 Main Street
East Hartford, Connecticut 06108

In reply please refer to:
KWB:dla:(0669k); MS 163-09
Ref. No. NASA CR-180861 (PWA-5967-46)

September 8, 1988

To: National Aeronautics and Space Administration
Lewis Research Center
21000 Brookpark Road
Cleveland, Ohio 44135

Attention: Mr. Dale Hopkins, Program Manager
Mail Stop 49-8

Subject: Structural Tailoring of Advanced Turboprops (STAT) Interim Report

Reference: Contract NAS3-23941

Attachments: Two Copies of Subject Report, NASA CR-180861 (PWA-5967-46)

Mr. Chamis:

We are pleased to submit the STAT Interim Report in compliance with terms of the reference contract.

Sincerely yours,

UNITED TECHNOLOGIES CORPORATION
Pratt & Whitney Group
Commercial Engineering

Kenneth W. Brown
Program Manager

cc: Administrative Contracting Officer
Air Force Plant Representative Office
UTC/Pratt & Whitney Group
East Hartford, Connecticut 06108

NASA National Aeronautics and Space Administration

Report Documentation Page

1. Report No.	2. Government Accession No.	3. Recipient's Catalog No.
NASA CR-180861		

4. Title and Subtitle	5. Report Date
Structural Tailoring of Advanced Turboprops (STAT) Interim Report	August 1988
	6. Performing Organization Code

7. Author(s)	8. Performing Organization Report No.
K. W. Brown	PWA-5967-46
	10. Work Unit No.

9. Performing Organization Name and Address	11. Contract or Grant No.
UNITED TECHNOLOGIES CORPORATION Pratt & Whitney 400 Main Street East Hartford, CT 06108	NAS3-23941
	13. Type of Report and Period Covered
12. Sponsoring Agency Name and Address National Aeronautics and Space Administration Lewis Research Center 21000 Brookpark Road Cleveland, OH 44135	Interim Report
	14. Sponsoring Agency Code

15. Supplementary Notes

Project Manager: D. A. Hopkins
NASA-Lewis Research Center, Cleveland, OH

16. Abstract

This interim report describes the progress achieved in the Structural Tailoring of Advanced Turboprops (STAT) program which was developed to perform numerical optimizations on highly swept propfan blades. The optimization procedure seeks to minimize an objective function, defined as either direct operating cost or aeroelastic differences between a blade and its scaled model, by tuning internal and external geometry variables that must satisfy realistic blade design constraints.

This report provides a detailed description of the input, optimization procedures, approximate analyses and refined analyses, as well as validation test cases for the STAT program. In addition, conclusions and recommendations are summarized.

17. Key Words (Suggested by Author(s))	18. Distribution Statement
Approximate Analysis; Mathematical Optimization; Objective Function; Refined Analysis	

19. Security Classif. (of this report)	20. Security Classif. (of this page)	21. No. of pages	22. Price
Unclassified	Unclassified	58	

NASA FORM 1626 OCT 86

Table of Contents

Section		Page
1.0	SUMMARY	1
2.0	INTRODUCTION	3
3.0	OVERVIEW	5
4.0	INPUT	6
4.1	Aerodynamic Stage	6
4.2	Support Structure	6
4.3	Operating Conditions	6
4.4	Materials	7
4.5	Objective Function	7
4.6	Constraints	8
4.7	Design Variables	8
5.0	OPTIMIZATION PROCEDURES	9
5.1	General Optimization Theory and Background	9
5.2	STAT ADS Implementation	11
5.3	Optimizer Comparison	14
5.4	Estimated Function Call Requirements	14
5.5	ADS Interface with STAT Approximate Analyses	15
6.0	APPROXIMATE ANALYSES	17
6.1	Aerodynamic Analysis (Efficiency)	17
6.2	Acoustic Analysis of Near-Field Noise	17
6.3	Blade Model Generation	18
6.3.1	Finite Element Mesh	18
6.3.2	Attachment Model	19
6.3.3	Equivalent Properties Generation	19
6.4	Finite Element Analysis	19
6.5	Postprocessing of Finite Element Output	21
6.6	Supersonic Flutter Analysis	22
6.7	Once-Per-Revolution Forced Response Analysis	23
6.8	Objective Functions	23
6.8.1	Direct Operating Cost	23
6.8.2	Aeroelastic Scale Model Tailoring	24
7.0	REFINED ANALYSES	26
7.1	Aerodynamic Analysis	26
7.2	Acoustic Analysis	26
7.3	Finite Element Analysis	26
7.4	Flutter Analysis	26

Table of Contents (continued)

Section		Page
8.0	STAT VALIDATION CASES	27
8.1	The Infeasible 18E LAP Design	27
8.2	The SR-7 LAP Design	37
8.3	The Aeroelastic Scale Model - The SR-7a	45
9.0	CONCLUSIONS AND RECOMMENDATIONS	49
10.0	REFERENCES	50
DISTRIBUTION LIST		51

List of Illustrations

Figure Number	Title	Page
1	Structural Tailoring of Advanced Turboprops overall program flow.	2
2	Feasible region is union of all points that satisfy all constraints.	10
3	STAT program flow.	16
4	Composite construction of the 18E blade.	28
5	18E external design curve definition - thickness/chord distribution.	28
6	18E external design curve definition - chord/diameter distribution.	29
7	18E external design curve definition - camber/lift coefficient distribution.	29
8	18E external design curve definition - blade twist distribution.	30
9	18E external design curve definition - conical section angle distribution.	30
10	18E external design curve definition - radial stacking distribution.	31
11	18E external design curve definition - tangential stacking distribution.	31
12	18E external design curve definition - axial stacking distribution.	32
13	Initial and optimum design composite construction overlay plots of the 18E blade.	35
14	Design curve overlays of 18E initial and optimum designs - blade twist distribution.	35
15	Design curve overlays of 18E initial and optimum designs - tangential stacking distribution.	36
16	Design curve overlays of 18E initial and optimum designs - axial stacking distribution.	36

List of Illustrations (continued)

Figure Number	Title	Page
17	Design curve comparison overlays of the 18E and SR-7 designs - thickness/chord distribution.	38
18	Design curve comparison overlays of the 18E and SR-7 designs - chord/diameter distribution.	38
19	Design curve comparison overlays of the 18E and SR-7 designs - camber/lift coefficient distribution.	39
20	Design curve comparison overlays of the 18E and SR-7 designs - blade twist distribution.	39
21	Design curve comparison overlays of the 18E and SR-7 designs - tangential stacking distribution.	40
22	Design curve comparison overlays of the 18E and SR-7 designs - axial stacking distribution.	40
23	Composite construction of the SR-7a.	45
24	Initial and optimum design composite construction overlay plots of the SR-7a.	48

List of Tables

Table Number	Title	Page
I	ADS Strategy Options	11
II	ADS Optimizer Options	12
III	ADS One-Dimensional Search Options	12
IV	ADS Program Options	13
V	ADS Optimization Algorithm Comparison	14
VI	Frequency Comparisons, STAT Finite Element Models	18
VII	STAT 18E and SR-7 Design Constraints	33
VIII	The 18E STAT Optimization Results	34
IX	The SR-7 STAT Optimization Results; Large Variable Test Case	41
X	The SR-7 STAT Optimization Results; Blade Restack to Solve Violated Stress Constraint	43
XI	Refined Versus Approximate Analyses for the Initial and Optimum SR-7 Designs	44
XII	The SR-7a STAT Optimization Results	46

SECTION 1.0

SUMMARY

The Structural Tailoring of Advanced Turboprops (STAT) computer program was developed to perform numerical optimizations on highly swept propfan blades. The optimization procedure seeks to minimize an objective function, defined as either direct operating cost or aeroelastic differences between a blade and its scaled model, by tuning internal and external geometry variables that must satisfy realistic blade design constraints.

The STAT analyses include an aerodynamic efficiency evaluation, a finite element stress and vibration analysis, an acoustic analysis, a flutter analysis, and a once-per-revolution (one-p) forced response life prediction capability. The STAT constraints include blade stresses, blade resonances, flutter, tip displacements and one-p forced response life. The STAT variables include all blade internal and external geometry parameters needed to define a composite material blade. The STAT objective function is dependent upon a blade baseline definition which the user supplies to describe a current blade design for cost optimization or for the tailoring of an aeroelastic scale model.

To perform a blade optimization, three component analysis categories are required: an optimization algorithm; approximate analysis procedures for objective function and constraint evaluation; and refined analysis procedures for optimum design validation. The STAT computer program contains an executive control module, an optimizer, and all necessary approximate and refined analyses. The optimization algorithm of STAT is the Automated Design Synthesis (ADS) optimization package, which is a proven tool for optimizations with a small to medium (1 to 30) number of design variables. A flowchart of the STAT procedure is shown in figure 1.

The approximate analyses of STAT utilize an efficient, coarse mesh, plate finite element blade vibration analysis procedure. The finite element analysis provides blade natural frequencies and mode shapes, stress under centrifugal and pressure loads, and blade weight. Additional constraint evaluations, including flutter, power, acoustic and one-p calculations, utilize output from the finite element analysis.

After each completed design optimization, the current design is verified by applying refined analyses to ensure that all constraints are satisfied. If the constraints are not all satisfied, then correction factors are applied to the approximate analysis results to better calibrate them with the refined analyses. The optimization process continues to the next completed design move until a local optimum design has been found whose constraints satisfy refined analyses.

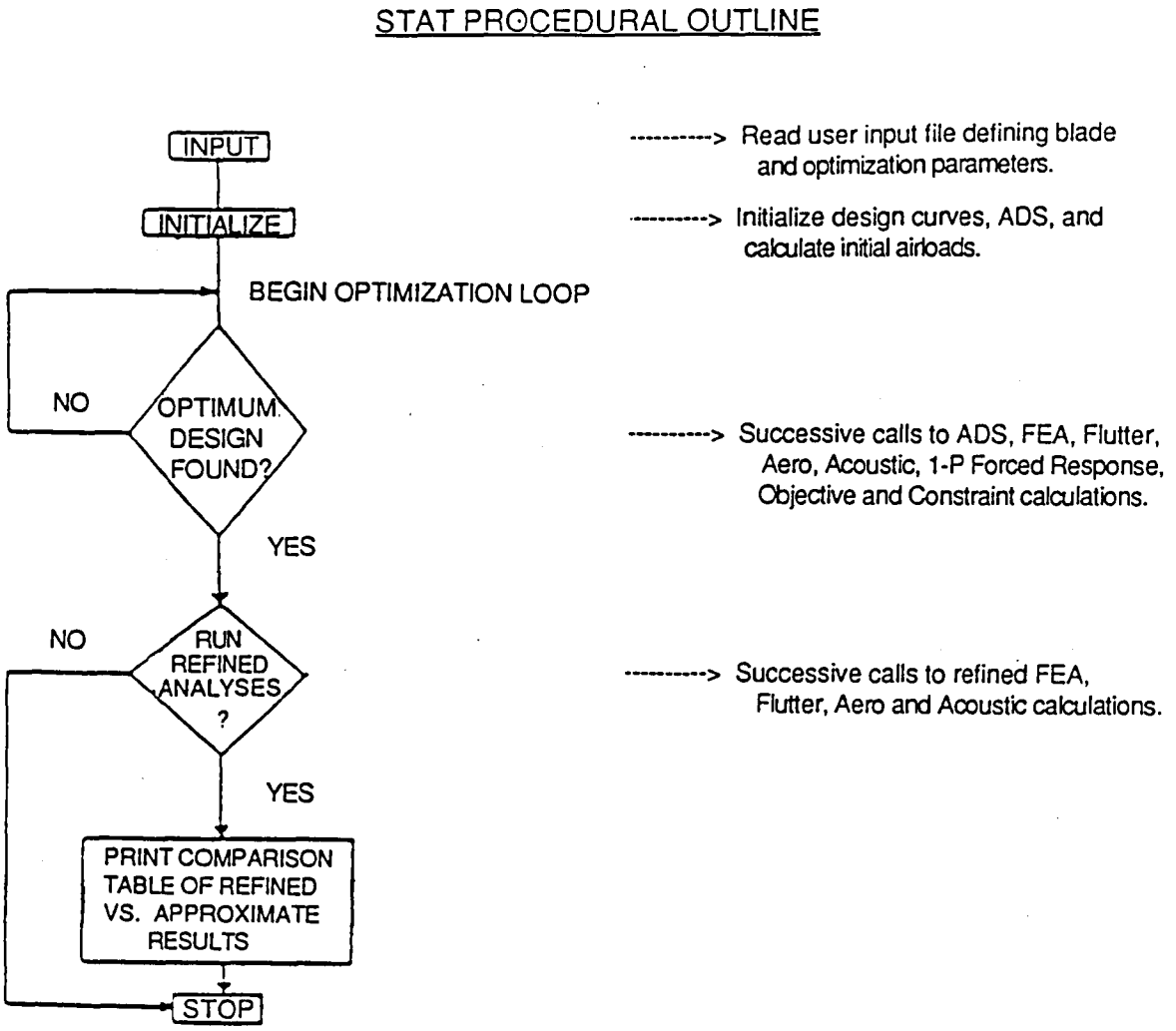

Figure 1. Structural Tailoring of Advanced Turboprops overall program flow.

To use the blade optimization system, design curves used to describe the external and internal geometry of the turboprop fan blade must be defined. External geometry curves define blade thickness, section stacking, camber, chord, twist and conical sections. Internal geometry curves define individual composite layer thickness, percent chord coverage and position over the entire blade.

The STAT system has been applied to the Large-Scale Advanced Prop-Fan (LAP) SR-7 blade, the LAP SR-7 aeroelastic scale model blade and the 18E SR-7 infeasible blade design. The STAT program made significant improvements in all three cases and demonstrated the great potential for design enhancements through the application of numerical optimization to turboprop fan blades of composite construction.

SECTION 2.0

INTRODUCTION

As a result of the rapid rise in fuel costs during the 1970s, a major thrust of the aeronautics community has been to reduce aircraft fuel consumption. Past studies conducted by NASA, Pratt & Whitney and Hamilton Standard have indicated that an advanced turboprop can play a significant role in this effort by reducing fuel consumption approximately 15 to 30 percent below the consumption level of today's turbofan engines. The turboprop blades, which operate in a very complicated and severe aero-mechanical environment, are highly swept and have low aspect ratios.

The swept turboprop design process involves applying state-of-the-art interdisciplinary engineering technologies in a complex procedure. Numerous design iterations are required to satisfy all design constraints and also to maintain high system performance. Currently, the key analytical and design decisions are made manually by engineers typically from several different design groups, thus making the iterative blade design process very expensive and time consuming. When a design that meets the analysis allowables is found, the design process is usually halted, even though the final design is not likely to be the best design possible within the scope of existing technology.

Thus, advanced turboprops promise performance improvement, proper structural integrity, reduced noise levels, and substantial reduction in direct operating cost over conventional turbofans. Using current design procedures, however, it is very difficult to arrive at a satisfactory turboprop design, much less an optimum one, due to the multi-iterative, manual inter-group design process that is required.

The current design procedure is partly engineering and partly art. The quality of the design is often the result of the judgement and experience of the engineers performing the various tasks. The accompanying penalties of less than optimum designs are long design times, low performance, and high noise and weight levels which ultimately result in increased aircraft operating cost. Resolution of these cost penalties may be reflected in a long development cycle requiring repeated design improvements.

Recent advances by Pratt & Whitney and NASA in automated fan blade tailoring have indicated that through design system automation, optimization procedures may be employed to provide intelligent design trade decisions in highly complicated engineering environments. The Structural Tailoring of Advanced Turboprops (STAT) contract has created a turboprop optimization system which can be used to automatically and efficiently improve candidate turboprop designs, find feasible design configurations, and refine these configurations to determine optimal designs which minimize aircraft direct operating cost. The STAT procedure can reduce human error and increase productivity in the propfan design process by automating what was formerly a cumbersome, judgmental design process.

To meet the objective of the STAT program, seven technical tasks were established as part of NASA Contract NAS3-23941:

Task I - Requirements: The requirements to be imposed on the selection of the approximate and refined analysis methods (Task II) and optimization methods (Task III) were determined.

Task II - Analytical Methods: Analytical methods identified through a survey of the literature and in-house sources were evaluated, and one approximate method and one refined method were selected to be used to develop the structural tailoring procedures of Task IV.

Task III - Optimization Methods: An evaluation of optimization methods was conducted to select at least two distinct methods to be used to develop the formal structural tailoring procedures under Task IV.

Task IV - Structural Tailoring Procedure Development: Under this task, the structural tailoring system was designed, and the software architecture and formal structural tailoring procedure were developed. The procedure was demonstrated by determining the optimum configuration for two propfan blades.

Task V - Dedicated Approximate Analysis: The approximate analysis methods used in Task IV were assessed and a plan prepared to develop a set of dedicated approximate analyses. The approximate analyses, included as software modules, were developed, incorporated into the system developed in Task IV, and then verified by reanalyzing the optimized blade designs.

Task VI - Procedural Refinement: The performance of the structural tailoring system with the dedicated approximate analyses was evaluated, and a plan to refine the procedure was developed based on this evaluation. All changes necessary to implement this plan were made to the system. Improvements made to the structural tailoring procedure were verified by reanalyzing the turboprop design selected in Task IV.

Task VII - Demonstration and Documentation: The structural tailoring system, including all approximate analyses, was delivered, installed and demonstrated at NASA-Lewis Research Center (LeRC). Final documentation, including a theoretical manual, user's manual, and a programmmer's manual were prepared. A seminar was held at NASA-LeRC to instruct attendees on the use of the STAT system.

The facility used for the STAT program development was an IBM SYSTEM 370 computing system. STAT was written in FORTRAN 77 for machine independence and has been successfully executed on the NASA-LeRC CRAY XMP-1 facility.

The capabilities of the automated propfan design procedure have been demonstrated through its application to swept propfan blades of advanced, composite construction, as well as to the design of an aerodynamic scale model blade. The design optimization of these complex structures was a rigorous test of the STAT procedure.

SECTION 3.0

OVERVIEW

To perform a successful blade optimization, three component analysis categories are required: an optimization algorithm; approximate analysis procedures for objective function and constraint evaluation; and refined analysis procedures for constraint recalibration and optimum design validation. The optimization algorithm of STAT is the Automated Design Synthesis (ADS) optimization package of reference 1. The ADS program offers a wide variety of optimization procedures, and is a well accepted and proven optimization tool for applications involving a small to medium (1 to 30) number of design variables.

Due to the number of design iterations required to achieve an optimum blade configuration, many blade analyses must be performed. To derive candidate optima as efficiently as possible, blade optimizations are performed using approximate analysis procedures. These approximate procedures are efficient, fast running, and reasonably accurate. As STAT searches for a candidate optimum, the results of the approximate analyses for each design move are calibrated against more complex, refined analyses. When the approximate and refined analyses agree within a prescribed tolerance, the design is a valid optimum. Should they disagree, the approximate analysis must be recalibrated, and the optimization process must be continued from the most recent design iteration results. It is possible that the refined and the approximate analyses would not show increased agreement even after recalibration. This would mean that the approximate analysis was neglecting an important design parameter, and, as such, should be improved or replaced.

The STAT finite element analysis uses NASTRAN's plate finite element technology so as to accurately represent the blade geometry for a large deflection, geometric nonlinear analysis. The plate element more accurately models blade effects such as uncamber and chordwise deflections when compared with beam models. It has been demonstrated with linear finite element analyses that relatively coarse plate meshes yield improved approximate analysis results at run times competitive with beam analysis procedures. The STAT approximate analyses must be self-contained; therefore, NASTRAN was not a viable approximate analysis option. Hence, a self-contained finite element analysis using NASTRAN plate element technology was constructed. Although the STAT finite element procedure uses NASTRAN technology, because of its reduced scale all matrices are stored in the core of the computer, and all procedures take place in core as well. Thus, for the small problems of the STAT approximate analyses, the special finite element computer code is able to deliver NASTRAN accuracy, but at greatly reduced computer expense.

SECTION 4.0

INPUT

Following are descriptions of the various categories of input information that must be provided to the STAT program.

4.1 AERODYNAMIC STAGE

The starting point for the structural tailoring of a turbo propfan blade is a candidate aerodynamic stage design. The geometry of the initial design is input to the structural tailoring procedure in the following form:

- Aerodynamic definitions at various sections along the airfoil radial axis (used to define airflow conditions, stagger, camber, twist, chord and thickness, all of which are functions of radius)
- Airfoil cross-sectional shape
- Number of blades.

4.2 SUPPORT STRUCTURE

The dominant variables which control structural tailoring are frequency dependent and sensitive to blade attachment flexibility. The attachment of an advanced turboprop design consists of the extended spar being retained in the hub by a ring of ball bearings. STAT approximates the attachment design as being cantilevered at the hub interface and having a circular cross-section. The required input is:

- Radius of the circular cross-section
- Length of the extended spar.

4.3 OPERATING CONDITIONS

Performance optimization requires the definition of the operating conditions for a specific propfan running position, typically design cruise. The required input is:

- Propeller operating environment (includes altitude, free-stream velocity, temperature and wake geometry)
- Propeller speed.

4.4 MATERIALS

Blade centrifugal stresses and vibratory characteristics result from body loads and are, therefore, fully dependent upon the properties of the blade materials. Blade life is dependent on the strength of the material subjected to a particular stress condition. The composite airfoils to be tailored in this program consist of laminates of bonded discrete composite plies. These plies consist of a fixed ratio of fiber and matrix components, and can be treated as equivalent homogeneous materials with directional properties. Similarly, adhesively bonded plies of metal matrix composite material can be considered to be an equivalent homogeneous material. The net criticality of a local stress state is determined by evaluating a parameter which is a function of the relative criticality of each individual ply stress state. The input which defines the required properties for each material (ply) is:

- Density
- Directional moduli and Poisson's ratios
- Directional static strength
- Directional cyclic strengths
- Ply orientation angle.

Additionally, a planform of ply coverage is required for the equivalent properties generator of the STAT analysis to generate equivalent finite element laminate material properties. This planform is input as a ply-by-ply table of ply location and width as fractions of chord, input at various sections along the airfoil radial axis.

4.5 OBJECTIVE FUNCTION

The STAT procedure optimizes a single benefit which can be related to the final design. To the engine operator the benefit may either be the total value, which is predominantly measured by aerodynamic performance, or the aeroelastic discrepancies of a scale model. The benefit expression is kept in generalized form by introducing a FORTRAN definition of:

- An objective function of design variables or quantities which are defined by the design variables (constant terms are not required).

4.6 CONSTRAINTS

The durability objectives of a blade design are accomplished by imposing limits on the quantities that are calculated in the structural analyses. Margins are established relative to idealized limits to recognize the effects of geometric, material, and operational tolerances and to compensate for approximations in the analyses or underlying assumptions. Input to the STAT procedure is:

- Maximum allowable blade tip uncamber, untwist, and axial deflections
- Minimum allowable difference between predicted frequencies and critical multiples of prop speed (engine order)
- Maximum allowable once-per-revolution forced response stress condition for each material (individual composite ply)
- Limits on various geometric design variables (to guarantee airfoil fabricability and erosion resistance)
- Turboprop required output power
- Minimum allowable predicted classical flutter Mach number and stall flutter parameter.

4.7 DESIGN VARIABLES

Airfoil cross-sectional shapes are used within the STAT procedure to vary the coordinates that define any airfoil section in proportion with changes to thickness, chord, camber, twist and stacking. Logic has also been included to identify the particular material at any point in a composite blade by references to quantities which define the relative position of the limits of coverage for that material. A fiber orientation angle is associated with each composite ply. Relevant inputs are coded identification of design variables and initial values for starting the iteration and include:

- Airfoil type (NACA Series Type)
- Blade thickness, chord, camber, twist and stacking
- Attachment length and diameter
- Composite material (ply) location and area coverage
- Composite material fiber orientation angles.

SECTION 5.0

OPTIMIZATION PROCEDURES

A common engineering design problem is the determination of values for design variables which minimize a design quantity such as weight, drag, or cost, while satisfying a set of auxiliary conditions. In the STAT program, the structural design of a composite swept turboprop blade is accomplished by varying airfoil section thicknesses, chord, fiberglass shell thickness, etc. to minimize a combination of weight and cost subject to constraints on resonance, flutter, stress, and foreign object damage.

5.1 GENERAL OPTIMIZATION THEORY AND BACKGROUND

The engineering design process can be modeled as a mathematical programming problem in optimization theory. In theoretical terms, this constrained minimization problem can be expressed as follows:

$$\text{minimize } f(x), \tag{1}$$

subject to the auxiliary conditions,

$$g_i(x) < 0, \; i=1, \ldots, m. \tag{2}$$

The quantity $x = (x1, \ldots, xn)$ is the vector of n design variables. The scalar function to be minimized, $f(x)$, is the objective function; and $g_i(x) < 0$, $i=1, \ldots, m$ are the m inequality constraints. Upper and lower bounds on the design variables, e.g.,

$$L_i < x_i < U_i, \; i=1, \ldots, n, \tag{3}$$

are referred to as side constraints. The n-dimensional space spanned by the design variables defines the design space. If $f(x)$ and $g_i(x)$, $i=1, \ldots, m$, are all linear functions of x, the optimization problem is a linear problem (LP) which can be solved by well known techniques, such as Dantzig's simplex method. If $f(x)$ or any of the $g_i(x)$'s are nonlinear, then it is a nonlinear programming (NP) problem for which a number of solution techniques are also available. If the objective function, $f(x)$, is to be maximized, then the equivalent problem of minimizing $-f(x)$ is performed.

Any choice of variables, x, in design space that satisfies all the constraints, equations (2) and (3), is a feasible point. As shown in figure 2, the union of all feasible points comprises the feasible region. The locus of points which satisfies $g_i(x) = 0$ for a particular i, forms a constraint surface. On one side of the surface, $g_i(x) < 0$ and the constraint is satisfied; on the other side, $g_i(x) > 0$ and the constraint is violated. Points on the interior of the feasible region are free points; points on the boundary are bound points. If it is composed of two or more distinct sets, the

feasible region is disjoint. A design point in the feasible region that minimizes the objective function is an optimal feasible point and is a solution of the problem posed in equations (1) through (3). As in any nonlinear minimization problem, there can be multiple local minima. In this case, the global minimum is the optimal feasible point. If a design point is on a constraint surface (i.e., $g_i(x) = 0$ for some i), then that particular constraint is active. A solution to a structural optimization problem is almost always on the boundary of the feasible region, and is usually at the intersection of two or more constraint surfaces (i.e., there are two or more active constraints).

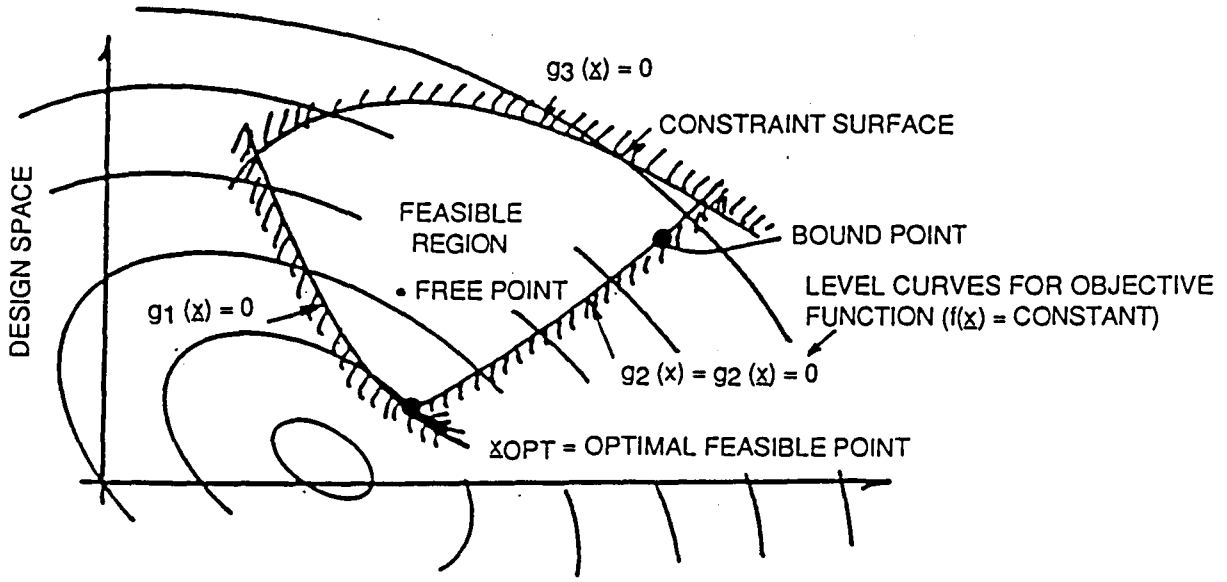

Figure 2. Feasible region is union of all points that satisfy all constraints.

There are two basic approaches to solving the constrained optimization problem posed in equations (1) through (3): direct methods (e.g., methods of feasible directions) and indirect methods (e.g., penalty function methods).

In a direct method, the objective function and constraints are evaluated independently, and the constraints are treated as limiting surfaces. Zoutendijk's method of feasible directions is an example of a direct method.

In an indirect method, the problem is reformulated so that equations (1) through (3) are replaced by a single unconstrained optimization problem. For example, in an exterior penalty function method, violations of the constraints are added onto the objective function to form an augmented objective function. If a constraint is violated, a penalty term is added onto the objective function. By minimizing the objective function subject to increasing values of

the penalty parameter, the optimum may be obtained. One advantage of this approach is that each of the successive minimization problems can be solved using a standard unconstrained function minimization technique, such as a conjugate gradient or quasi-Newton method. Computationally, however, the process is not usually competitive with direct procedures.

Many optimization software packages are available in software libraries (e.g., IMSL = International Mathematical and Statistic Libraries, Inc., and HARWELL) that can solve the constrained minimization problem using either direct or indirect techniques. Due to its proven success and versatility in solving structural optimization problems at Pratt & Whitney, NASA-Langley, General Motors, Ford, and other locations, the Automated Design Synthesis (ADS) computer program was selected for the STAT blade optimization application. The ADS program (ref. 1) is a general optimization package developed by G. N. Vanderplaats of Engineering Design Optimization, Inc. for NASA-Langley.

5.2 STAT ADS IMPLEMENTATION

ADS is a general purpose numerical optimization program containing a wide variety of optimization algorithms. The solution of the optimization problem has been divided into three basic levels by ADS: (1) strategy, (2) optimizer, and (3) one-dimensional search. By allowing the user to personally select the strategy, optimizer, and one-dimensional search procedure, considerable flexibility is provided for finding an optimization algorithm which works well for the specific design problem being solved.

Strategy

The optimization strategies available in STAT are listed in Table I. The parameter ISTRAT is sent to the ADS program to identify the strategy selected by the user. Selecting the ISTRAT=0 option transfers control directly to the optimizer. This is selected when choosing the Method of Feasible Directions or the Modified Method of Feasible Directions for solving the constrained optimization problem.

TABLE I. ADS STRATEGY OPTIONS

ISTRAT	Strategy to be Used
0	None. Go directly to the optimizer.
1	Sequential unconstrained minimization using the exterior penalty function method.
2	Sequential unconstrained minimization using the linear extended interior penalty function method.
3	Sequential unconstrained minimization using the quadratic extended interior penalty function method.
4	Sequential unconstrained minimization using the cubic extended interior penalty function method.
5	Augmented Lagrange Multiplier Method.
6	Sequential Linear Programming.
7	Method of Centers.
8	Sequential Quadratic Programming.
9	Sequential Convex Programming.

Optimizer

The IOPT parameter selects the optimizer to be used by ADS. Table II lists the optimizers available within STAT. Note that not all optimizers are available for all strategies. Allowable combinations are shown on Table IV.

TABLE II. ADS OPTIMIZER OPTIONS

IOPT	Optimizer to be Used
1	Fletcher-Reeves algorithm for unconstrained minimization.
2	Davidon-Fletcher-Powell (DFP) variable metric method for unconstrained minimization.
3	Broydon-Fletcher-Goldfarb-Shanno (BFGS) variable metric method for unconstrained minimization.
4	Method of Feasible Directions for constrained minimization.
5	Modified Method of Feasible Directions for constrained minimization.

One-Dimensional Search

Table III lists the one-dimensional search options available for unconstrained and constrained optimization problems. The parameter ISERCH selects the search algorithm to be used.

TABLE III. ADS ONE-DIMENSIONAL SEARCH OPTIONS

ISERCH	One-Dimensional Search Option
1	Find the minimum of an unconstrained function using the Golden Section method.
2	Find the minimum of an unconstrained function using the Golden Section method followed by polynomial interpolation.
3	Find the minimum of an unconstrained function by first finding bounds and then using polynomial interpolation.
4	Find the minimum of an unconstrained function by polynomial interpolation/extrapolation without first finding bounds on the solution.
5	Find the minimum of a constrained function using the Golden Section method.
6	Find the minimum of a constrained function using the Golden Section method followed by polynomial interpolation.
7	Find the minimum of a constrained function by first finding bounds and then using polynomial interpolation.
8	Find the minimum of a constrained function by polynomial interpolation/extrapolation without first finding bounds on the solution.

Allowable Combinations of Algorithms

Not all combinations of strategy, optimizer, and one-dimensional search are meaningful. For example, it is not meaningful to use a constrained one-dimensional search when minimizing unconstrained functions. Table IV identifies those combinations of algorithms which are meaningful in the STAT program. In this table, an X is used to denote an acceptable combination of strategy, optimizer, and one-dimensional search; while an 0 indicates an unacceptable choice of algorithm. To use the table, start by selecting a strategy. Read across to determine the admissable optimizers for that strategy. Then, read down to determine the acceptable one-dimensional search procedures. From the table, it is clear that a large number of possible combinations of algorithms is available.

TABLE IV. ADS PROGRAM OPTIONS

	Optimizer				
Strategy	1	2	3	4	5
0	X	X	X	X	X
1	X	X	X	0	0
2	X	X	X	0	0
3	X	X	X	0	0
4	X	X	X	0	0
5	X	X	X	0	0
6	0	0	0	X	X
7	0	0	0	X	X
8	0	0	0	X	X
9	0	0	0	X	X
One-Dimensional Search					
1	X	X	X	0	0
2	X	X	X	0	0
3	X	X	X	0	0
4	X	X	X	0	0
5	0	0	0	X	X
6	0	0	0	X	X
7	0	0	0	X	X
8	0	0	0	X	X

X = Acceptable
0 = Not Acceptable

5.3 OPTIMIZER COMPARISON

A simplistic comparison of the optimization algorithms available to the ADS program was conducted by optimizing a simple beam. The problem is to minimize the weight of a rectangular cross-section cantilever beam under bending load, subject to bending stress, shear stress, aspect ratio, and deflection constraints. A sample of the options available in the ADS program was run, as detailed in Table V. As can be seen from the table, the feasible directions and the modified feasible directions procedures are among the most efficient optimization algorithms yet developed. This trend has also applied to the STAT optimizations conducted to date.

TABLE V. ADS OPTIMIZATION ALGORITHM COMPARISON

ISTRAT	IOPT	ISERCH	Funct. Calls	Min. Wt.
0	4	7	21	6763
0	4	5	46	6525
0	5	5	43	6637
0	5	6	43	6637
0	5	7	29	6603
0	5	8	23	6574
1	1	8	62	8451
2	1	8	134	7440
3	1	8	137	7426
4	1	8	26	20000
5	1	8	55	10102
5	2	8	52	7445
5	3	8	56	7336
6	4	8	24	6613
6	5	8	24	6626
7	5	8	33	7548
8	5	8	34	6476
9	5	8	33	6757

5.4 ESTIMATED FUNCTION CALL REQUIREMENTS

A reasonable estimate for the number of analysis function calls, and hence the amount of computer time that will be required, may be made based on experience with the ADS optimizer and STAT. As indicated in figure 2, each optimizer design iteration consists of a gradient evaluation of the objective function and constraints to determine the search direction, followed by a one-dimensional line search in that direction. When the gradients are not known analytically (as is the case for the STAT system), a backward difference gradient approximation is used. For n design variables, n function calls are required for the finite difference gradient calculation.

Method of Feasible Directions

The one-dimensional line search usually requires three additional function evaluations to update the objective function and constraints and to determine where the search should terminate. Thus, for m iterations, with n+3 function calls per iteration, we have:

$$N = m\ (n + 3)\ , \tag{4}$$

where N is the number of function evaluations required to determine the optimum design. Typically, convergence is attained in approximately 10 iterations, so that a good estimate for function call requirements is N = 10 * n + 30. Notably, N increases linearly with an increase in the number of design variables.

Modified Method of Feasible Directions

The modified method of feasible directions tends to follow the actual constraint surface more closely than does the method of feasible directions, and hence requires fewer design iterations, often converging in 4 or 5 iterations. This is done at the sacrifice of more moves along the one-dimensional line search, often taking 8 or 10 of these. In all, a reasonable estimate for function call requirements for this method is N = 6 * n + 50. Thus, for relatively large problems, this procedure promises to be more economical than the method of feasible directions. In practice, it is often useful to test each method, for at times one will achieve a superior design than the other, regardless of function call requirements.

5.5 ADS INTERFACE WITH STAT APPROXIMATE ANALYSES

The various STAT approximate analyses and the ADS optimizer are all called from the STAT executive routine. The output from ADS to the analyses is in the form of a design vector. This vector contains changes to the design variables. These changes are splined and added to the design curves, which are then used in the flutter, finite element, and other analyses. These analyses provide values that are used to calculate an objective function value and constraint values, which are used by ADS to determine the next design vector. This process continues until an optimum is reached. The overall program flow is detailed in figure 3.

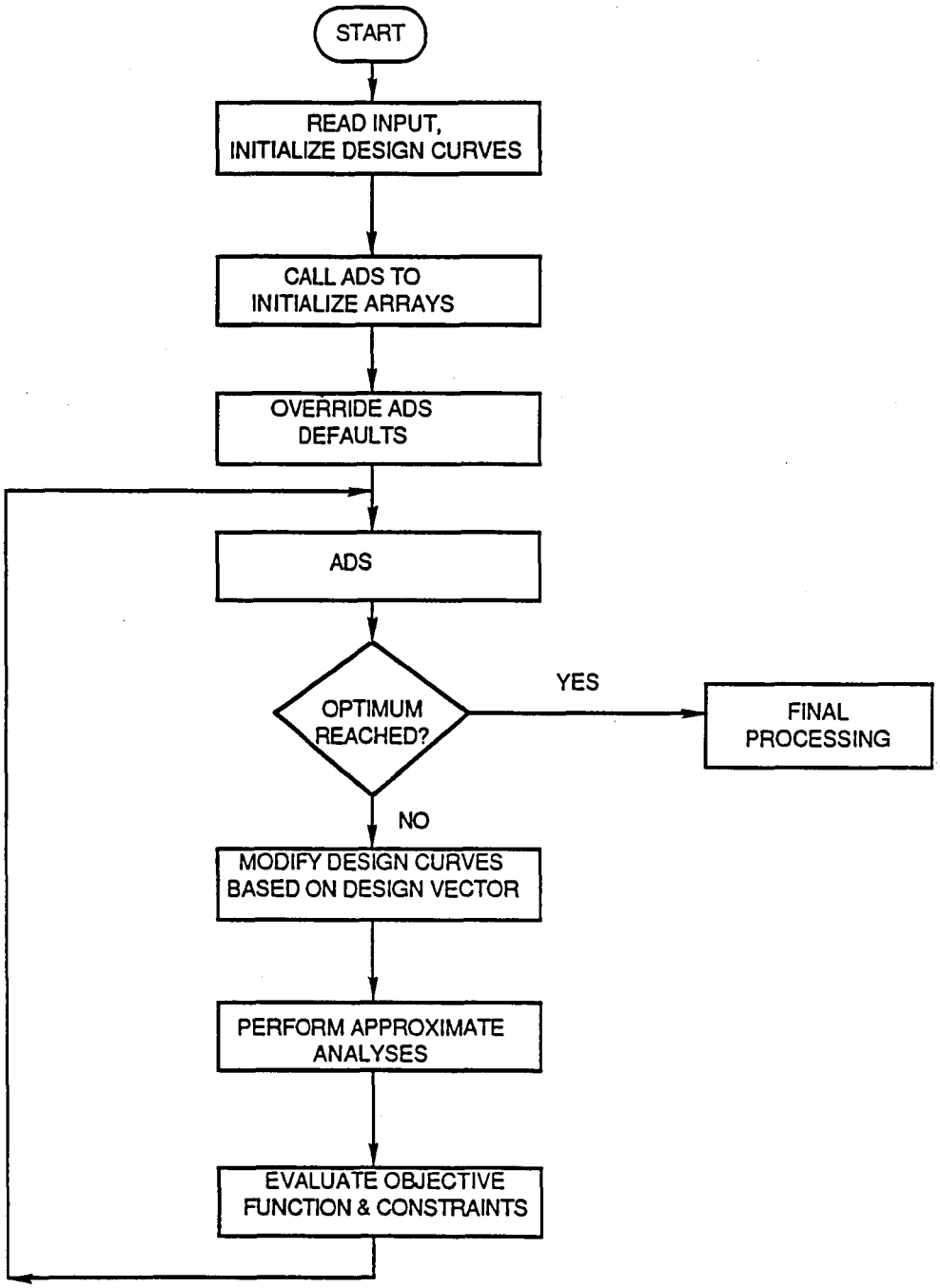

Figure 3. STAT program flow.

SECTION 6.0

APPROXIMATE ANALYSES

6.1 AERODYNAMIC ANALYSIS (EFFICIENCY)

The module used to calculate propeller efficiency is a high-speed propeller-nacelle aerodynamic performance method (ref. 2). The method uses lifting line theory, with a swept bound segmented vortex, and prescribed trailing segmented vortices. The induced velocity from each vortex segment can be expressed, using the Biot-Savart equation, as a function of vortex segment position, field point and the vortex strength. Through a matrix inversion, blade circulation and induced velocity are solved.

The method contains compressible features for blade induction and blade profile losses. The law of forbidden signals corrects the induced velocity when relative Mach numbers are greater than one. The compressible two-dimensional airfoil data used are also corrected for Mach numbers greater than one by applying a Mach Cone correction (ref. 3). Additionally, the analysis is performed on the hot running position of the blade and is therefore called after the finite element analysis has been completed.

6.2 ACOUSTIC ANALYSIS OF NEAR-FIELD NOISE

Two forms of acoustic emissions are relevant to propfan design, namely far-field noise and near-field noise. The far-field noise is of concern primarily during takeoff and landing to establish community noise levels and to comply with noise certification requirements. Typically, the far-field noise is system dependent, and cannot be improved by the design variables available within STAT, and hence has not been considered in the STAT system. Near-field noise has a direct effect on the aircraft weight, and hence the fuel burned, since fuselage acoustic treatment (more weight) is required to achieve acceptable cabin noise levels when near-field noise is high.

The Hamilton Standard proprietary acoustics analysis encompasses near-field and far-field noise and is based on the Hanson frequency domain propfan noise theory. Unfortunately, this detailed acoustic analysis consumes too much computer time for application to the STAT optimization procedure. Instead, an approximate near-field noise analysis was developed which calculates the maximum free-field noise level of the blade passage frequency tone at the fuselage through a data base interpolation. Trends were developed by exercising the Hamilton Standard theoretical noise prediction computer program, varying parameters most sensitive to noise (e.g., tip speed, power loading, flight Mach number, number of blades, diameter and blade sweep). These trends were then tabulated to provide a data base. Sound pressure levels are derived from the data base using multiple levels of interpolation in the tables.

Despite the fact that the approximate acoustic module does not recognize all details of blade design, it does contain trends for those parameters having major effects on the near-field noise level during design cruise conditions. Thus, the curve fit accuracy is adequate for identifying trends during blade optimization and represents STAT's approximate near-field noise analysis package. The table lookup technique has shown good correlation with refined acoustic analyses for operating conditions that range from 15 to 40 SHP/D**2 (shaft-hp/diameter-squared), 600 to 800 fps blade tip speed and 0.60 to 0.85 Mach number. Noise levels for operating conditions that are outside these ranges are calculated from linear extrapolation of the correlated data.

One powerful means for reducing the near-field noise is to introduce blade sweep. Sweeping the blades, either forward or aft, introduces a phase shift along the blade span which promotes cancellation of emissions.

6.3 BLADE MODEL GENERATION

Due to the high number of approximate finite element analyses performed by the STAT system, efficient mesh generation is important. Additionally, the accuracy of mesh generation aids refined analysis calibration, and provides proper gradient information for the optimization scheme.

6.3.1 Finite Element Mesh

To arrive at an economical, yet accurate, approximate finite element propfan representation, a combination of a coarse mesh with a selective pattern of master degrees-of-freedom (DOF) employed in the Guyan reduction procedure has been utilized. As shown in Table VI, the STAT approximate model, while using only 70 nodal points, is accurate within 2 percent for the frequencies of the first three modes, when compared with the more detailed STAT refined analysis of a typical propfan geometry.

TABLE VI. FREQUENCY COMPARISONS, STAT FINITE ELEMENT MODELS

Mesh	Grids	Master DOF	f1	f2	f3	f4
Approximate	10 x 7	24	29.6	71.6	121.0	150.1
Refined	20 x 10	64	30.2	70.0	122.0	133.0

Airfoil mesh generation requires the generation of coordinates and thicknesses for all grid point locations. The airfoil type is selected by the user in the input file. The geometry of each radial cross-section is scaled depending on blade thickness and chord. The suction and pressure surfaces of the blade are determined by splining several radial sections from the blade root to tip. Using the surface definitions, the meanline coordinates and thicknesses are calculated for each airfoil grid point location.

User desired station specifications for the mesh to be generated can be accomplished through the STAT input cards, SPANTAB and CHORDTAB. These cards directly supply the program with percent chord and percent span locations of the airfoil mesh gridpoints.

6.3.2 Attachment Model

For highly swept, propfan blades of spar-shell composite structure, the attachment is an extension of the spar and may usually be approximated as cylindrical in cross-section. Within STAT, the user has two options for defining the attachment section. When a shank length and diameter are specified, the program will automatically create the required model data, generating a finite element beam model of the blade attachment section. Optionally, the STAT attachment model can be defined using NASTRAN bulk data type input cards, using any combination of supported elements, including beams, springs and plates.

6.3.3 Equivalent Properties Generation

Equivalent properties for composite materials are generated in the mesh preprocessor, by applying lamination theory to the composite blade construction, while maintaining the blade aerodynamic profile. The layup is treated as symmetric through the thickness of the shell so that no coupling exists between the bending and membrane stiffnesses. Application of lamination theory (ref. 5) to the composite element yields effective stiffness arrays for membrane and for bending motions. These matrices are compatible with NASTRAN material descriptions for the plate elements employed.

6.4 FINITE ELEMENT ANALYSIS

Incorporation of finite element procedures into STAT for approximate analysis required employing the most efficient solution procedures available. NASTRAN finite element technology (ref. 4) was selected for use as the approximate analysis for several reasons:

1. Proven computational efficiency
2. Established successful correlations with test experience
3. Convenient, user-friendly input/output
4. Compatibility with NASTRAN refined analysis procedures.

The STAT finite element code has been generated specifically for propfan stress and vibration analysis. The program performs large deflection analyses using plate, beam, and spring elements. For a given rotor speed, the STAT finite element program performs a large deflection static solution, followed by a prestressed natural modes solution. Stresses, eigenvalues and eigenvectors are calculated.

Due to the limited scope of the STAT finite element code, it is possible to perform all solutions within the computer core, thus improving analysis efficiency. Thus, STAT plate analyses have become competitive with beam analyses in cost, but with significantly improved accuracy.

The STAT plate element is a reduced integration triangular plate finite element, which includes the following features:

1. Recognition of thickness taper
2. Properly stacked triangular plate element meshes to simulate airfoil pretwist and camber
3. Composite material capabilities (using lamination theory)
4. Element differential stiffness
5. Lumped masses are employed, ensuring a diagonal stiffness matrix, for storage efficiency.

The geometric nonlinear finite element analysis in STAT permits analysis of structures which undergo large deflections and rotations. Material linearity is maintained by requiring that the strains in any finite element remain small. In a linear static analysis all coordinate systems are assumed to be stationary with respect to an inertial frame. The nonlinear static analysis permits the local element coordinate system to translate and rotate relative to the reference frame. Whereas this coordinate system motion may be large, the relative element deflections must remain small. The relative element deflections are obtained through coordinate transformations. It is these transformations which introduce the geometric nonlinear relations.

The linear static analysis, a two step process, precedes the nonlinear solution. Step one of the linear static analysis includes assembling the structural stiffness, K, and external loads, P. Deflections, U1, are obtained through the product of the stiffness matrix inverse and the external load vector.

$$(U1) = | K |^{-1} (P)$$

Step two utilizes these deflections to produce a linear correction on the initial stiffness to account for the effect of load-deflection interaction. This correction is called the differential stiffness, Kd, and is used to modify the original stiffness, K. The second solution is obtained;

$$(U2) = | K + Kd |^{-1} (P)$$

The nonlinear solution process is simply an extension of the linear static procedure, and in fact builds on the prestressed linear static solution, U2. In simplest terms, the nonlinear solution involves an iterative process which converges when the external and internal loads are in equilibrium. The iteration process uses the previous solution vector to form an incremental element stiffness matrix and internal force vector. The incremental stiffness is combined with the initial stiffness similar to the differential stiffness procedure. Internal forces are then calculated from the product of the modified stiffness and the deflections. New external loads may be regenerated based upon the deflected shape. The difference of the external and internal load vectors multiplied by the inverse of the modified stiffness produces an incremental deflection vector. The incremental deflection vector magnitude approaches zero as force equilibrium is achieved.

The iteration process may be sped up by not rebuilding the stiffness matrix or the external load vector during each pass. This may result in more iterations being required to achieve a converged solution, but each iteration is faster due to fewer matrix operations. As the problem becomes more nonlinear, such "shortcuts" are not advisable. The nonlinear iteration process is successful only if the first solution is relatively close to the converged answer.

6.5 POSTPROCESSING OF FINITE ELEMENT OUTPUT

The STAT finite element code provides, as output, static displacements and stresses (for the composite equivalent elements), as well as at-speed eigenvalues, eigenvectors and modal equivalent stresses. Many of these data blocks must be postprocessed before they may be used either for constraint evaluation or as input to other subroutines. Element stresses must be converted to composite ply stresses for the static deformations and natural modes. Blade sectional mass properties must be evaluated from the assembled finite element mass matrix. Additionally, the flutter analysis requires frequency, mode shape, and generalized mass information.

The evaluation of static and modal composite blade ply stress values requires processing of the element stress values based upon the application of lamination theory (ref. 5). The lamination theory assumes that plane sections (through the plate thickness) remain plane after deformation. The laminate processor provides the matrices required to convert the element equivalent stresses to membrane and bending strains. Then, based on the lamination assumptions, ply strains are calculated, leading to ply stresses, and, ultimately, to the Tsai-Wu tensor failure theory equivalent stress evaluation (ref. 6).

The objective function for scale model tailoring requires the blade section mass distribution for comparison with the full blade mass properties. The full sized, assembled finite element mass matrix is used to evaluate the total mass at each radial station of the finite element blade by using a simple averaging scheme. The difference between the inertia properties of the blade and its scaled model is then evaluated.

The evaluation of flutter constraints requires that equivalent beam mode shapes be generated from the available plate mode shape data, due to the beam theory of the present flutter codes. Beam mode shapes are generated from the available plate mode shapes by performing a spline fit of each component of the mode shape on each cross section. From the spline fit, modal bending and torsional motions are determined at the section shear center, for transmittal to the flutter analysis.

6.6 SUPERSONIC FLUTTER ANALYSIS

Approximate Flutter Analysis Subroutine

The approximate flutter analysis in the STAT optimization analysis performs both the unstalled and stalled flutter calculations. Each flutter analysis procedure is described below.

Unstalled Flutter Analysis

The unstalled flutter stability subroutine was specifically tailored to model the structural and aerodynamic complexities of the propfan. The blade structure is represented by fully coupled mode shapes. The coupled modes take the form of translation normal to the blade surface at the mid-chord and rotations about the blade mid-chord. The mode shapes are passed to the subroutine from the finite element analysis routines. Unsteady airloads are formulated using strip theory with no induced velocities included. The blade is divided into a series of discrete aerodynamic panels of constant property. Each panel is defined with plunging and pitching about the mid-chord reference specified by the mode shape displacement definition. Unsteady, unstalled lift and moment equations for the two-dimensional panels are generalizations of the unsteady swept aerodynamic equations generated by Barmby, Cunningham and Garrick (ref. 7). The equations are modified to account for compressibility and sweep. Cascade effects are taken into account in the analysis with an empirical correction based on propfan model tests.

Stalled Flutter Analysis

The stalled flutter stability analysis is based on empirical data used to prevent torsional stall flutter of propeller blades. The blade mode shapes passed to the subroutine are examined to determine the torsion mode. The torsional frequency is then used to calculate a stall flutter parameter that must be greater than one for a given configuration to be free from torsional stall flutter.

Refined Flutter Analysis Subroutine

The refined flutter analysis in the STAT optimization analysis performs both the unstalled and stalled flutter calculations. The unstalled flutter analysis equations are upgraded to account for compressibility, sweep, and cascade effects. The stalled flutter analysis remains unchanged from the approximate algorithm.

6.7 ONCE-PER-REVOLUTION FORCED RESPONSE ANALYSIS

Due to the presence of resonance constraints, large vibratory stresses are in general avoided. One possible exception to this is in the case of once-per-revolution (1P) excitations. In flight, the engine axis may depart from the aircraft velocity vector by a yaw angle. Thus, in undergoing one revolution, the propeller will encounter a first harmonic variation of its aerodynamics, which can induce strong vibratory stresses.

The propeller once-per-revolution (1P) loads are calculated at a user-supplied airplane yaw angle. The method utilizes Goldstein induction theory (ref. 8) and the same compressible 2-D airfoil data used by the aerodynamic module to calculate the advancing and retreating blade peak-to-peak loads.

A modal forced response analysis is performed on the propfan using the first five system modes to determine modal vibratory stresses. Adequate fatigue life is assured by mapping the steady and vibratory ply equivalent stresses onto a Goodman diagram, and constraining the combination to be less than the material strength for every finite element over the entire blade. The axis intercept points for the fatigue diagram are taken to be a Tsai-Wu steady stress allowable of 1.0, and a Tsai-Wu vibratory stress allowable of 1.0, with linear combinations assumed for combined loads.

6.8 OBJECTIVE FUNCTIONS

STAT supports the definition of two unique objective functions. For optimizations of conventional propfans, the aircraft direct operating costs are determined to optimize blade performance parameters such as noise, efficiency and weight. For the tailoring of the geometry of an aeroelastic scale model propfan, the static and dynamic differences between a blade and its scale model are minimized.

6.8.1 Direct Operating Cost

The aircraft direct operating cost (DOC) is calculated from input aircraft sensitivity factors, and calculated values of propeller efficiency, aircraft fuselage noise level, and propeller weight. The sensitivity factors, obtained from aircraft or engine companies, vary with aircraft type, size and mission. The factors supplied for the STAT test cases are based on a 120 passenger, 0.8 Mach number, 1200 nautical mile, twin engine aircraft. Generalizations for propeller gearbox weight and acoustic treatment weight are approximations but are included in the DOC calculation. The DOC is calculated relative to a user-defined baseline propeller.

In STAT, the change in operating cost is taken as a weighted sum of change in cost due to changes in efficiency, propeller weight, acoustic treatment weight, acquisition cost, and maintenance cost. The weighting factors are input by the user, according to the following:

```
DDOC =      EFFIC * DOCE * 100 +
       +    (PROP WT) * DOCP / 1000 +
       +    (ACOUS WT) * DOCA / 2000 +
       +    (ACQUIS COST) * DOCCA / 100,000 +
       +    (MAINT COST) * DOCCM
```

where DOCE = Cost of efficiency, $/%
DOCP = Cost of propeller weight, $/(1000 lb)
DOCA = Cost of acoustic weight, $/ton
DOCCA = Cost of acquisition cost, $/($100000)
DOCCM = Maintenance cost, $/($ of maint).

6.8.2 Aeroelastic Scale Model Tailoring

The definition of the objective function for the tailoring of an aeroelastic scale model of a turboprop fan blade assumes that both the scaled model and the full blade:

1. Have the same tip speed
2. Experience the identical aerodynamic, environmental conditions
3. Have the identical external geometry shape.

With these assumptions, the objective function is structured so as to minimize the following relationships between the scaled and full blade:

(1) $$\sum_{i=1}^{nmd} \frac{(f_{B,i} - K*f_{s,i})^2}{f_{B,i}^2}$$ ... blade frequencies

(2) $$\sum_{i=1}^{nst} \frac{(M_{B,i} - K^3*M_{s,i})^2}{M_{B,i}^2}$$ ... mass distribution

(3) $$\sum_{i=1}^{nmd} \frac{[(\theta b/d)_{B,i} - (\theta b/d)_{s,i}]^2}{(\theta b/d)_{B,i}^2}$$ ... modal deflections

(4) $$\frac{(\phi_B - \phi_s)^2}{\phi_B^2}$$ ... static deflection

where:

nmd represents the number of modes
nst represents the number of blade stations
S represents the scale model
B represents the full-size blade
f is blade natural frequency
M is blade sectional mass
θ is blade modal tip torsional deflection
b is blade tip chord length
d is blade modal tip easywise bending deflection
$\emptyset$ is blade static tip untwist
k is the model scale factor.

The objective function is defined as the sum of the quantities (1) through (4). In the limit, as the objective function approaches zero, all aeroelastic differences between the full blade and its scale model are eliminated. How well the scale model blade represents the aeroelastic characteristics of the full-size blade depends on the depth of the comparisons made through the objective function and the accuracy of the analytical tools used by STAT. The tailored scale model blade will have similar flutter, resonance, efficiency, acoustic, and static and modal deflection characteristics, but because the internal structure of the blade is varied during the optimization process, stress distribution will not be comparable.

SECTION 7.0

REFINED ANALYSES

Upon completion of an approximate turboprop optimization, STAT conducts a verification of the feasibility of the optimum design, using refined analysis procedures. Should the design meet all design limits, then an acceptable, optimized design has been obtained. Should one or more of the design limits be violated, then the approximate analyses are recalibrated, and the approximate optimization is reinitiated. This analysis recalibration is accomplished either by using "correction factors" that are available for each defined constraint, or by manually altering the constraint allowables.

The STAT optimized design convergence process can obviously be enhanced by having accurate approximate analyses. To this end, STAT uses the most accurate, yet computer time efficient, analyses available for its approximate turboprop optimization procedures.

7.1 AERODYNAMIC ANALYSIS

The STAT refined aerodynamic analysis utilizes the same analysis as was performed for the approximate analysis, but with more radial stations for improved integration accuracy. A small incremental computational cost is incurred. The analysis is performed on the hot, deformed geometry.

7.2 ACOUSTIC ANALYSIS

The STAT refined acoustic analysis is a Hamilton Standard proprietary code. The current public version of STAT contains only a dummy refined acoustic module.

Also, certain geometric details of the blade design (thickness, chord, twist, sweep distribution, etc.) are considered in the refined acoustic analysis that are not considered in the approximate analysis. This is considered a valid approach because when blade design details are varied within the typical range of propfan blade designs, their importance to noise at the blade passage frequency is secondary to the effect of parametric variations that include operating conditions, number of blades, and sweep.

7.3 FINITE ELEMENT ANALYSIS

The STAT refined finite element analysis is the same analysis procedure as the approximate finite element analysis, but with a more detailed mesh. Due to computer storage limitations, the current version of STAT uses a 12 node x 9 node breakup for the refined blade model. If a more detailed mesh is desired, the user can specify the mesh size desired, and the mesh generator will process the mesh, which can in turn be run in the NASTRAN code outside of the STAT analysis package.

7.4 FLUTTER ANALYSIS

The STAT refined flutter analysis is a Hamilton Standard proprietary code. The current public version of STAT contains only a dummy refined flutter module.

SECTION 8.0

STAT VALIDATION CASES

The STAT program has successfully demonstrated the potential of design optimization when applied to propfan blades of composite construction. STAT produced improved designs for both the SR-7 and 18E Large-Scale Advanced Prop-Fan (LAP) blades (ref. 9). Additionally, the optimizer proved to be capable of constructing an aeroelastic scale model representation of the SR-7 blade.

The tailorings of two turboprop blades were performed successfully using STAT. For these particular cases, the objective function was defined as the change in aircraft direct operating cost (DOC). The DOC was calculated from input aircraft sensitivity factors, and calculated values of propeller efficiency, aircraft fuselage noise level and propeller weight, all relative to the user-defined baseline performance of the SR-7 LAP blade. The sensitivity factors used to weight the different contributors apply to a 120 passenger, 0.8 Mach number, 1200 nautical mile, twin engine aircraft.

The two large full-scale propfan (LAP) blade designs that have been tailored by STAT are directly related to one another. The 18E LAP blade is one of the many preliminary designs (87th of a total of 100 design iterations) of the project from which the SR-7 LAP design evolved. The internal composite construction and material, the physical constraints of stress, flutter, power, and resonances, the aerodynamic environment and the blade attachment definitions were all identical for the two designs. However, the external geometry parameters (e.g., stacking, thickness, twist) of the blades were uniquely defined.

The third and final validation test case of the present STAT code was to construct an aeroelastic scale model representation of the SR-7 LAP design. The objective function for this optimization process was carefully thought out so that the model developed would take on the identical dynamic and static characteristics of the SR-7 design. The objective function calculated differences in blade mass distribution, static tip deflection, modal tip deflections and resonances.

8.1 THE INFEASIBLE 18E LAP DESIGN

The 18E LAP blade design is a preliminary design of the SR-7 which has high stress problems. The blade is of a composite construction incorporating a leading edge nickel sheath layer for protection against foreign object damage, a fiberglass outer shell, an internal aluminum spar, and foam used to fill the gaps between the spar and the shell to prevent localized shell buckling. The internal construction of the blade is shown in figure 4. The external geometry of the blade is defined by eight spanwise distribution curves that include blade stacking, twist, chord, thickness, and other pertinent parameters. Figures 5 through 12 summarize the external definition curves of the 18E blade design.

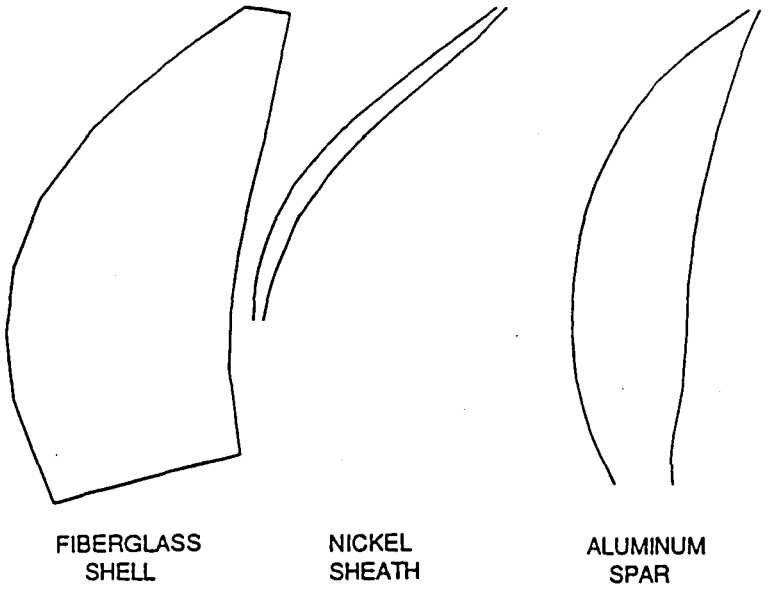

Figure 4. Composite construction of the 18E blade.

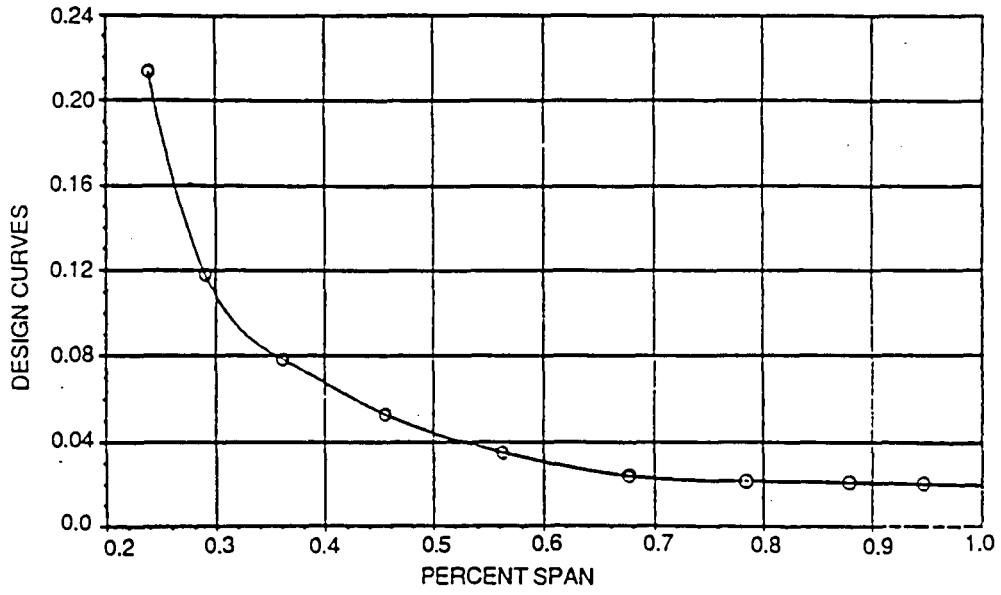

Figure 5. 18E external design curve definition - thickness/chord distribution.

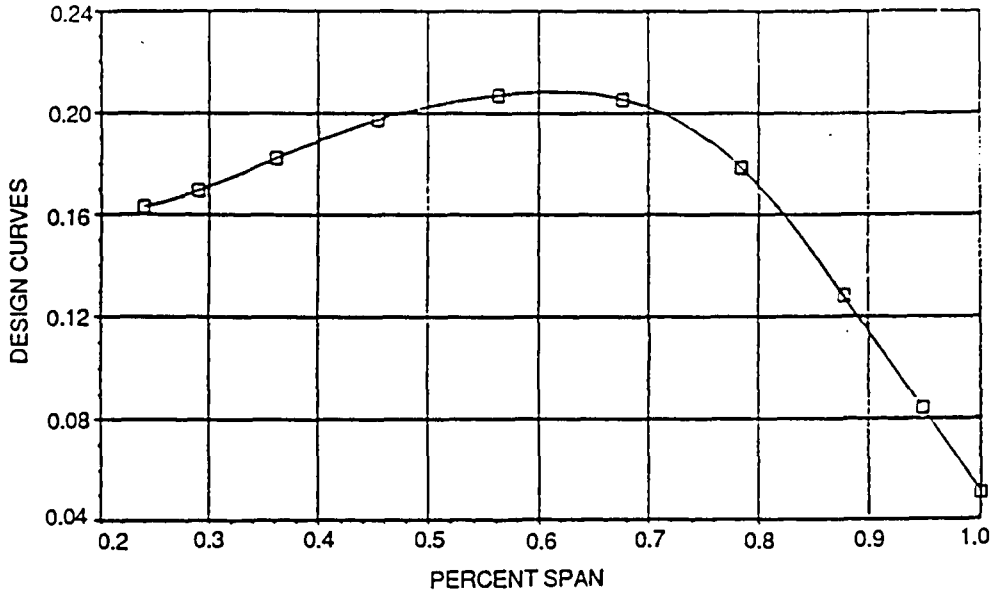

Figure 6. 18E external design curve definition - chord/diameter distribution.

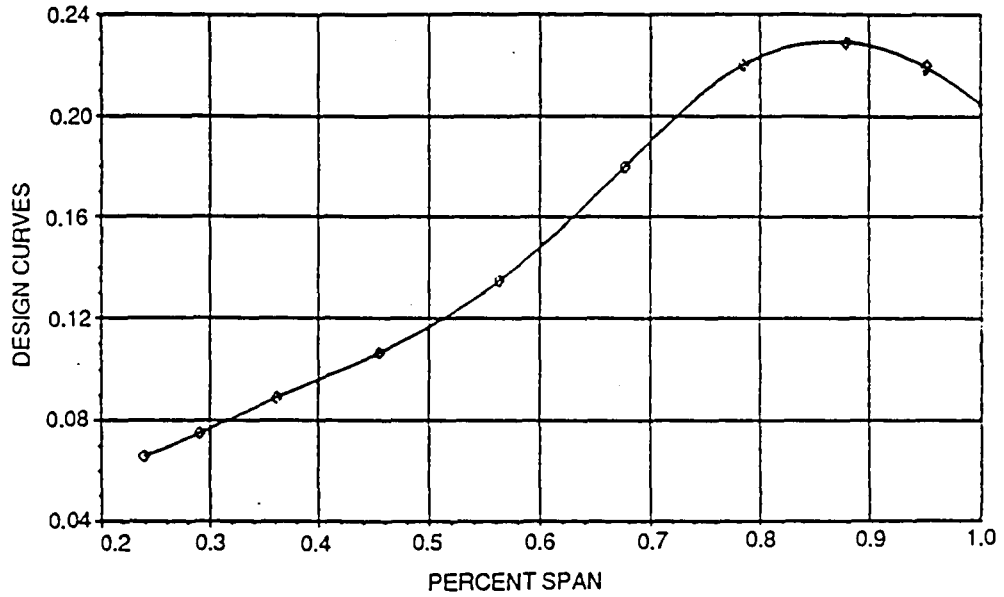

Figure 7. 18E external design curve definition - camber/lift coefficient distribution.

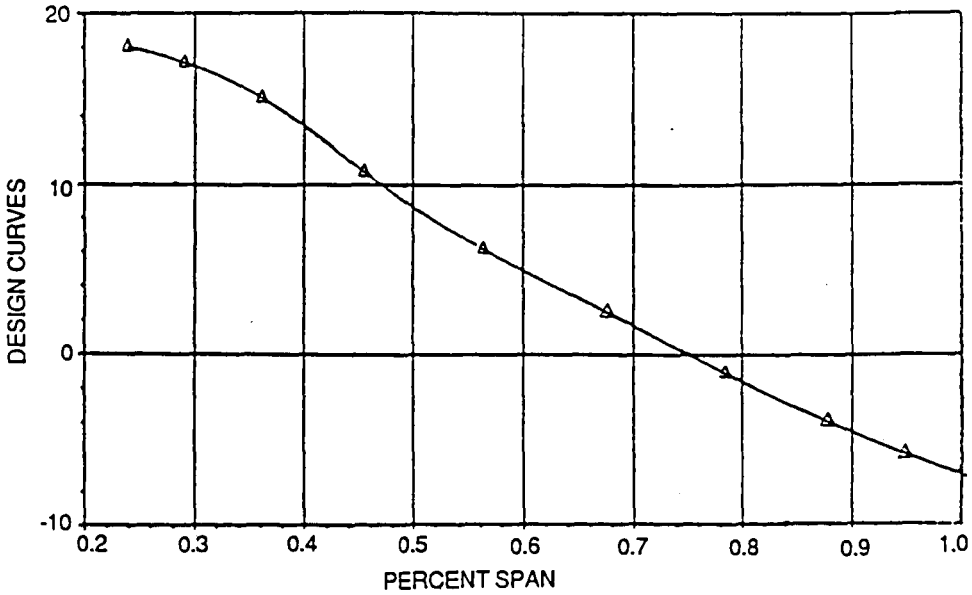

Figure 8. 18E external design curve definition - blade twist distribution.

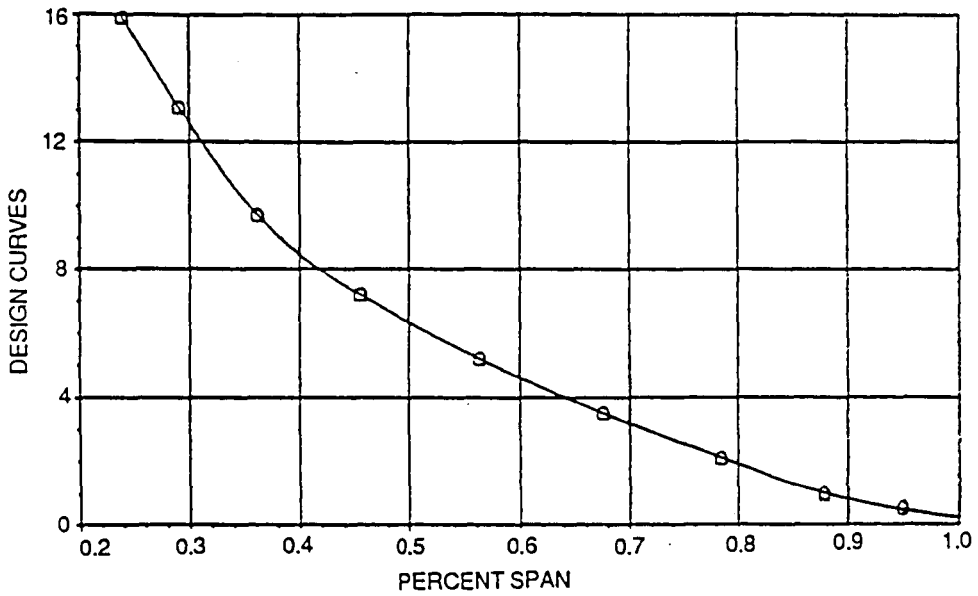

Figure 9. 18E external design curve definition - conical section angle distribution.

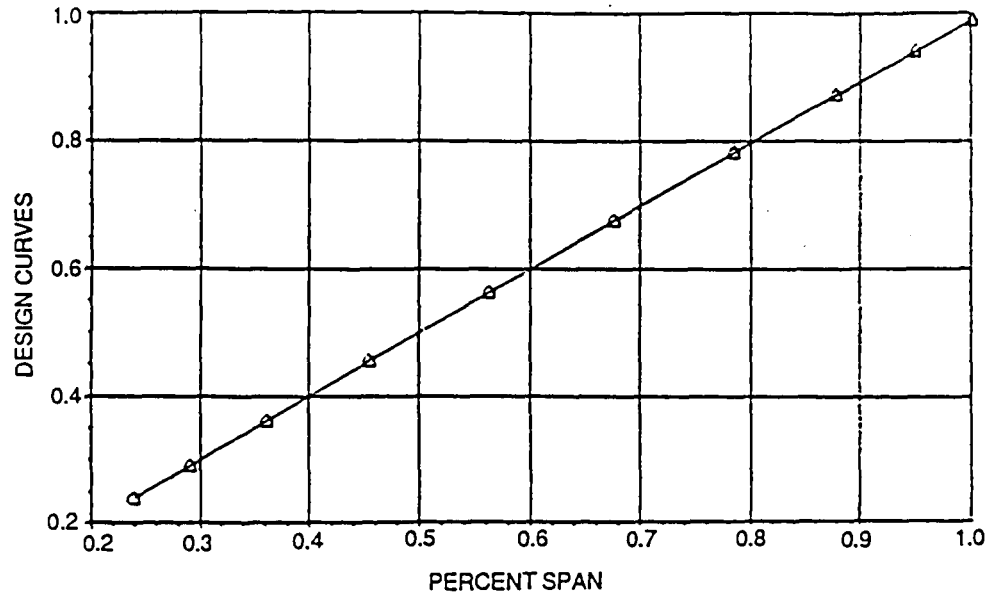

Figure 10. 18E external design curve definition - radial stacking distribution.

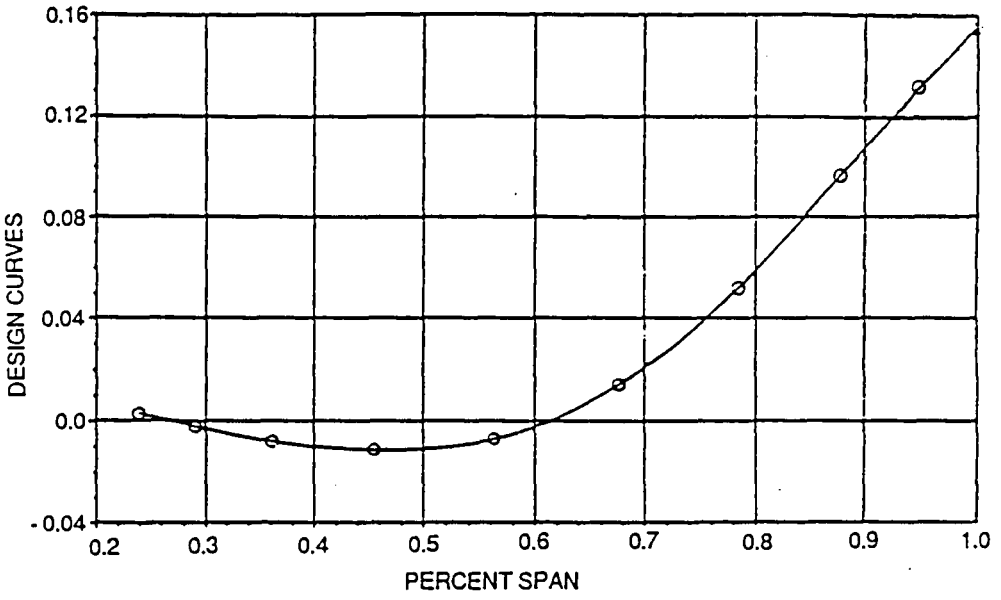

Figure 11. 18E external design curve definition - tangential stacking distribution.

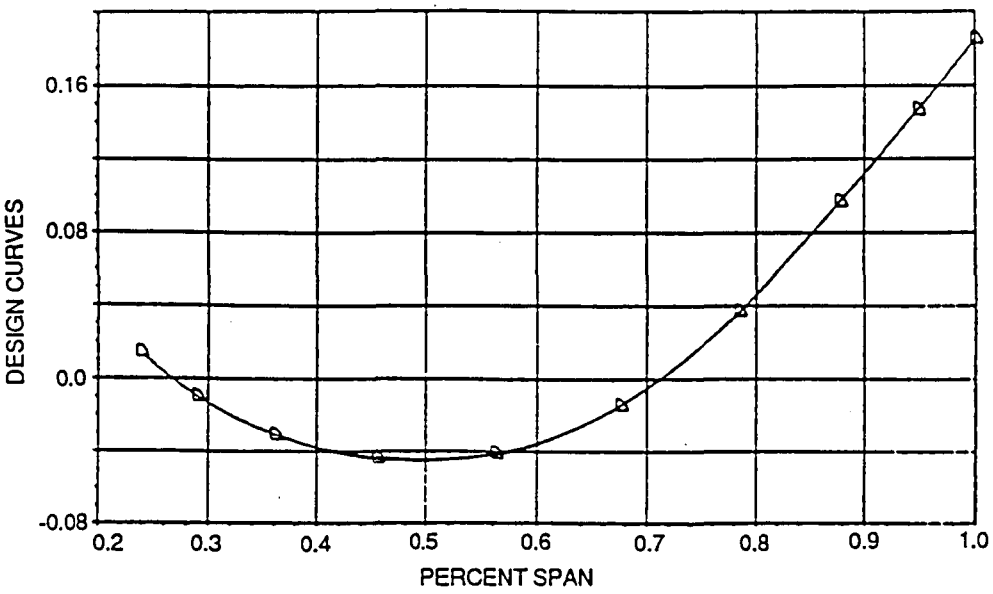

Figure 12. 18E external design curve definition - axial stacking distribution.

The 18E design constraints involve blade geometry tolerances, resonance margins, static stress, once-per-revolution force response life fraction, classical flutter Mach number, stall flutter and maintaining required driving power (equality constraint). The STAT 18E constraints are summarized in Table VII.

The variables used to optimize the 18E design included blade twist, axial stacking and tangential stacking. The stacking variables were used so as to solve the high stress problems, and the twist variables were used to maintain the power required to drive the propeller. The STAT variables and their blade locations are summarized in Table VIII. The values represent changes (deltas) from the baseline initial configuration.

The optimization results of the 18E design are quite impressive. After a total of 127 function calls, which included 8 complete design iterations, the STAT program produced a feasible design with a final DOC of 4.6 percent better than the current SR-7 LAP blade. This optimization analysis required 43 minutes of CPU on the Pratt & Whitney IBM 3090 mainframe computer. The blade's stress problems were solved in just two complete design moves but then, the power equality constraint became violated. The power constraint and all other constraints were satisfied after the fourth design move was completed. Over the final four design moves, STAT reduced the blade DOC by 3.4 percent and converged to an optimum design. The summary of the results is provided in Table VIII and figures 13 through 16.

TABLE VII. STAT 18E AND SR-7 DESIGN CONSTRAINTS

Blade Geometry

- Thickness/Chord minimums to avoid buckling
- Set realistic upper and lower boundaries for all variables
- Maintain root stacking position relative to the attachment

Blade Flutter

- Classical Flutter Mach number > 1.0
- Stall Flutter parameter > 1.0

Power

- Propfan driving power must be maintained at 2592 horsepower

Blade Resonance Margins

- 1st mode 2E - 10%
- 2nd mode 4E - 5%
- 2nd mode 5E - 2.5%
- 3rd mode 5E - 2.5%

Blade Stress

- Tsai-Wu layer steady stress < 1.0
- Once-per-revolution force response life fraction < 1.0

TABLE VIII. THE 18E STAT OPTIMIZATION RESULTS

Design Variables	Prescribed Delta Limits	Delta Achieved
Blade Twist Span Location:		
45.47%	-90 to 90 degrees	0.48106
67.62%	-90 to 90 degrees	0.15467
78.45%	-90 to 90 degrees	-0.84462
100.0%	-90 to 90 degrees	0.12180
Tangential Tilt Span Location:		
45.47%	-1.E+5 to 1.E+5 inches	-0.23042
67.62%	-1.E+5 to 1.E+5 inches	0.01163
87.80%	-1.E+5 to 1.E+5 inches	-1.18654
100.0%	-1.E+5 to 1.E+5 inches	0.72425
Axial Tilt Span Location:		
45.47%	-1.E+5 to 1.E+5 inches	-0.47834
67.62%	-1.E+5 to 1.E+5 inches	0.83312
87.80%	-1.E+5 to 1.E+5 inches	-1.00645
100.0%	-1.E+5 to 1.E+5 inches	0.18511

Design Constraints	Limits	Initial	Final
Resonances			
1st mode 2E	0.10 margin	-0.16285	-0.16685
2nd mode 4E	0.05 margin	-0.27795	-0.27713
2nd mode 5E	0.025 margin	-0.42236	-0.42171
3rd mode 5E	0.025 margin	-0.20416	-0.19155
Steady Stress (Tsai-Wu)			
sheath	1.0	2.06730	0.04884
shell	1.0	1.07049	0.03820
foam	1.0	0.10294	0.00277
spar	1.0	0.38873	0.00720
One-P Force Response			
Life Fraction	1.0	20.2960	0.48071
Flutter			
Flutter Mach Number	1.0	1.03080	1.1890
Stall Flutter	1.0	1.67140	1.5872
Driving Power	2592.	2592.	2596.3

Objective Function	Initial	Final
DOC:		
efficiency	-1.32996	-1.60311
noise	0.14850	-2.90490
weight	-0.03604	-0.03471
acquisition	-0.01632	-0.01572
maintenance	-0.00598	-0.00576
total =	-1.23980	-4.56420
Efficiency - (%)	82.206	83.266
Noise - (db)	143.82	137.35
Weight - (lb)	41.093	41.214

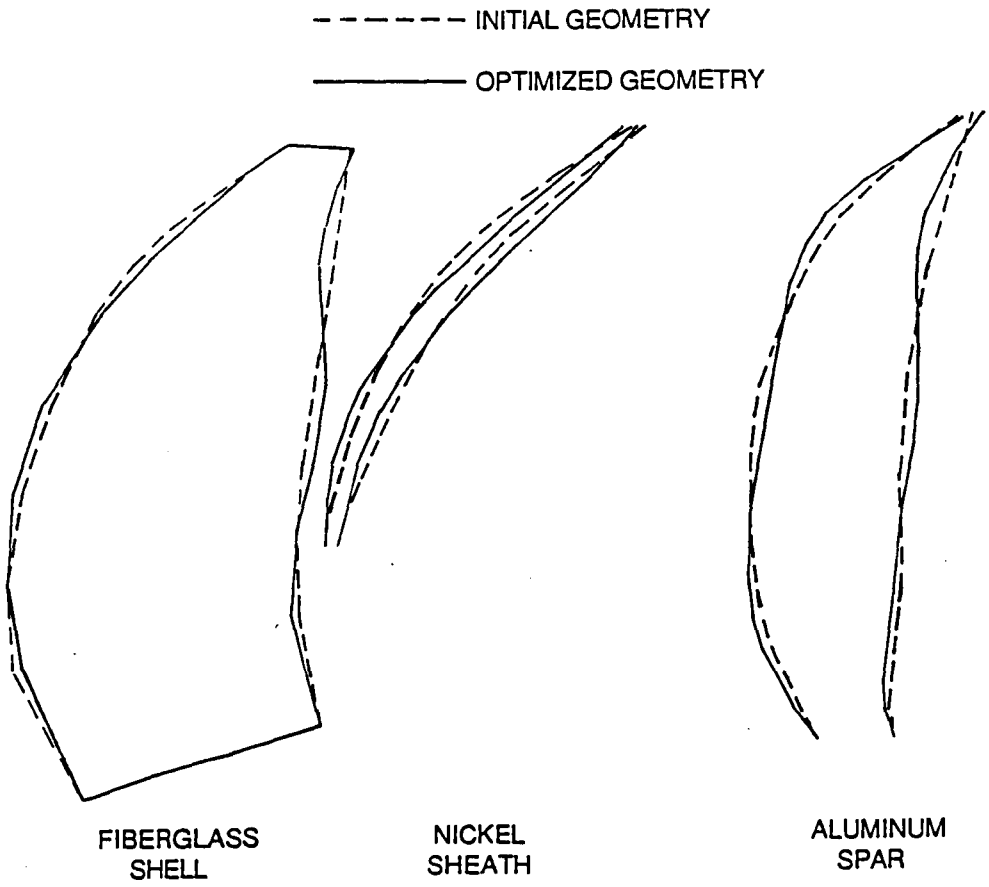

Figure 13. Initial and optimum design composite construction overlay plots of the 18E blade.

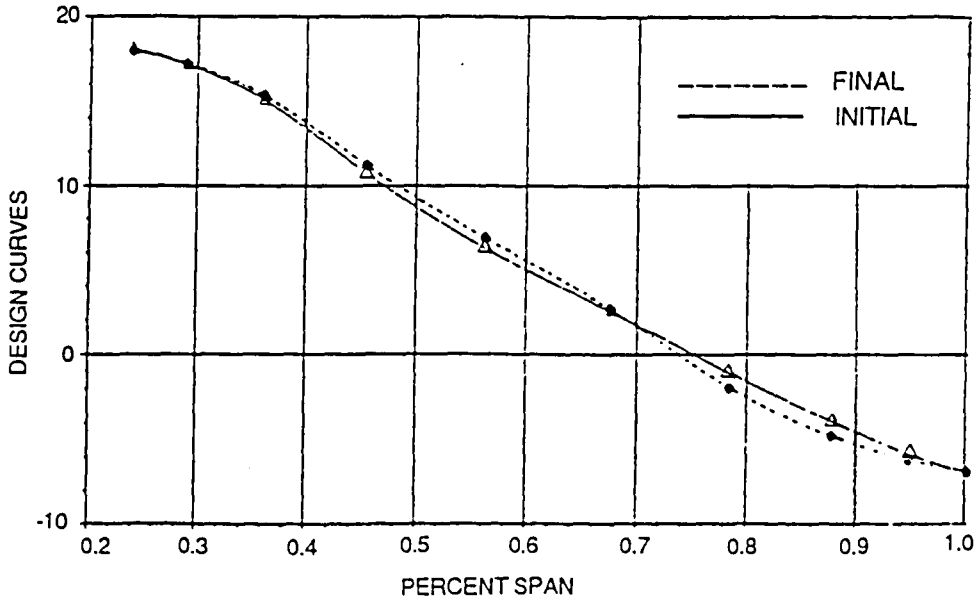

Figure 14. Design curve overlays of 18E initial and optimum designs - blade twist distribution.

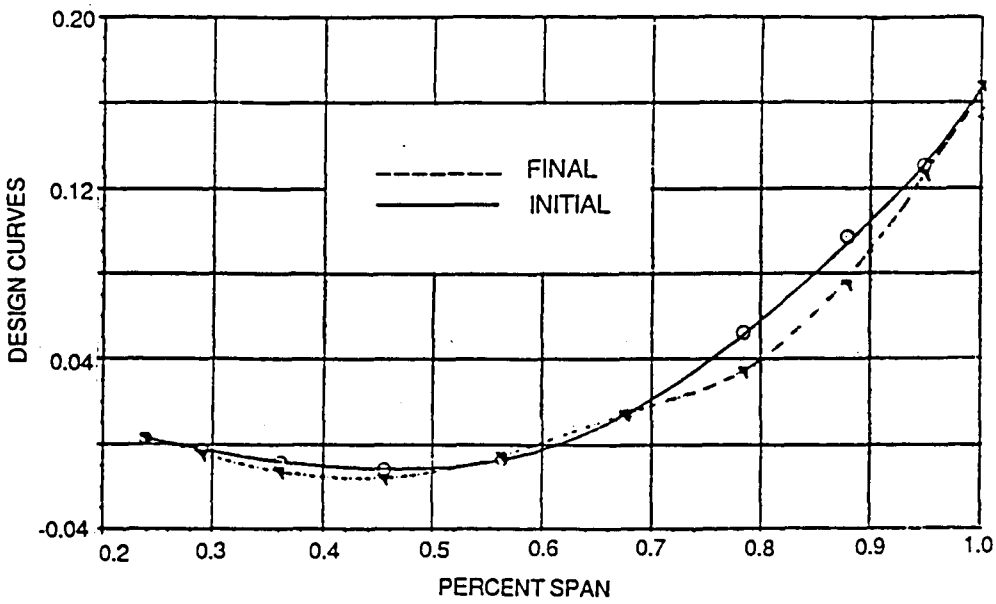

Figure 15. Design curve overlays of 18E initial and optimum designs - tangential stacking distribution.

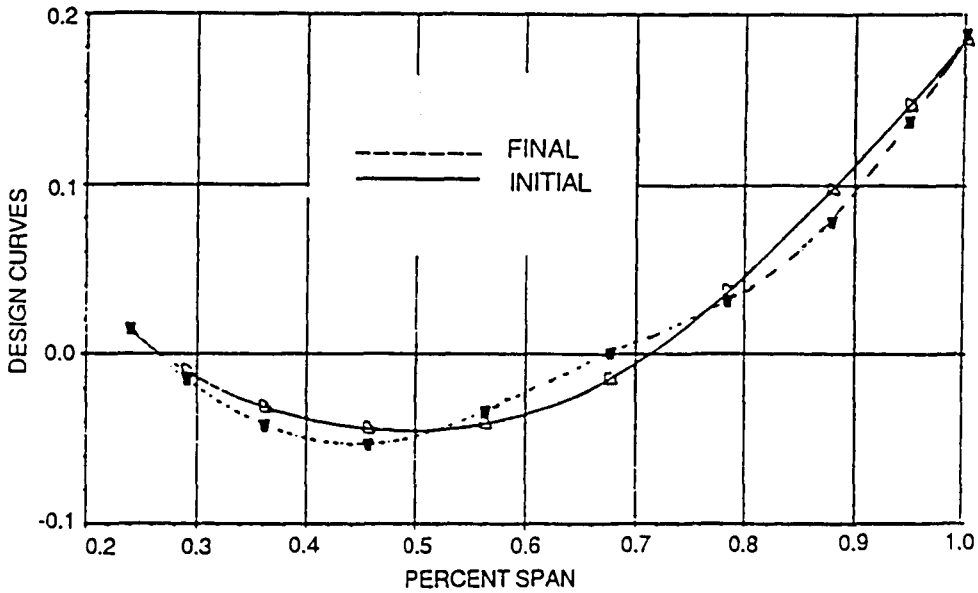

Figure 16. Design curve overlays of 18E initial and optimum designs - axial stacking distribution.

8.2 THE SR-7 LAP DESIGN

The SR-7 design has the identical internal composite construction of the 18E Prop-Fan (fig. 4), as well as the same design constraints (Table VII). The blade design differences arise with the external geometry definition. The SR-7 and 18E external geometry curves are provided for comparison in figures 17 through 22.

The SR-7 design was optimized using 38 variables which included most all of the parameters necessary to describe the blade. A list of the 38 variables used in the large variable test case is given in Table IX.

Unlike the 18E design, the SR-7 LAP blade initially satisfied all of the design constraints. For the large, 38 variable test case, the STAT optimizer was allowed to converge to an optimum design using the ADS algorithm 'modified method of feasible directions'. The final result was a LAP blade with a DOC improvement of 5.0 percent. However, this particular STAT test case unveiled one of several shortcomings to the new ADS autoscaling procedure. In scaled space, the once-per-revolution forced response life prediction constraint is only slightly violated, such that the optimizer classifies it as an active, not a violated constraint, and thus considers the design as acceptable. However, when the design space is unscaled, the measure of the constraint violation has changed in such a manner as to make it unacceptable.

Due to the violated one-p stress constraint, a second STAT optimization analysis was performed without the use of ADS autoscaling and using just 12 variables to restack the optimum blade from the prior optimization results to solve the stress problem. STAT was able to quickly find a feasible design.

Finally, the results of the STAT SR-7 optimization test case were analyzed using the refined codes for the aerodynamic, acoustic, flutter and finite element analyses so as to verify the optimum design. From Table XI, it is obvious that the approximate acoustic analysis is not properly predicting near-field noise trends for changes in blade design. Nevertheless, all of the constraints have remained satisfied and the final refined design blade DOC shows a 3.0 percent improvement over the initial SR-7 design. The STAT SR-7 test case results are compiled in Tables IX through XI.

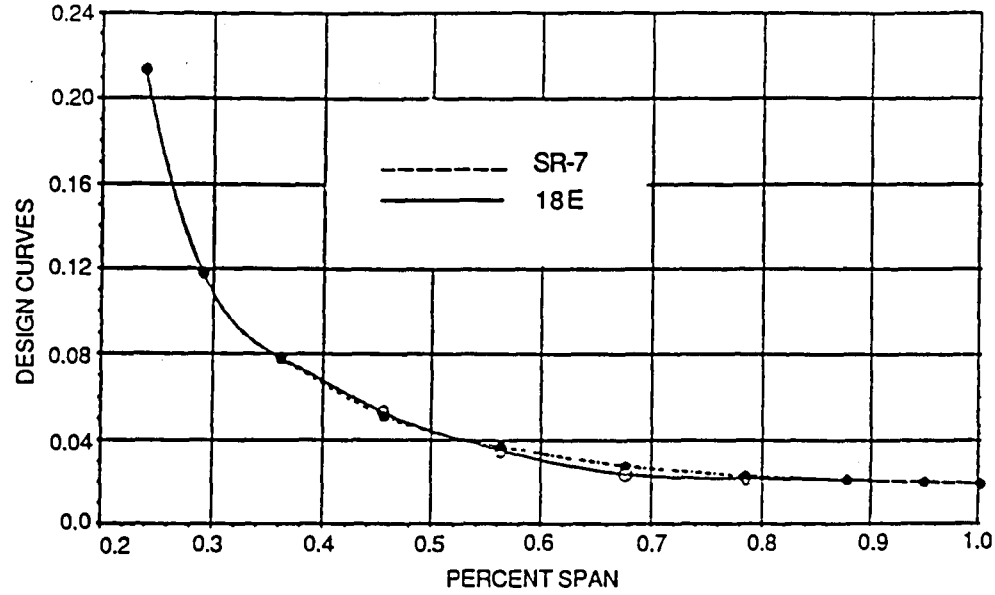

Figure 17. Design curve comparison overlays of the 18E and SR-7 designs - thickness/chord distribution.

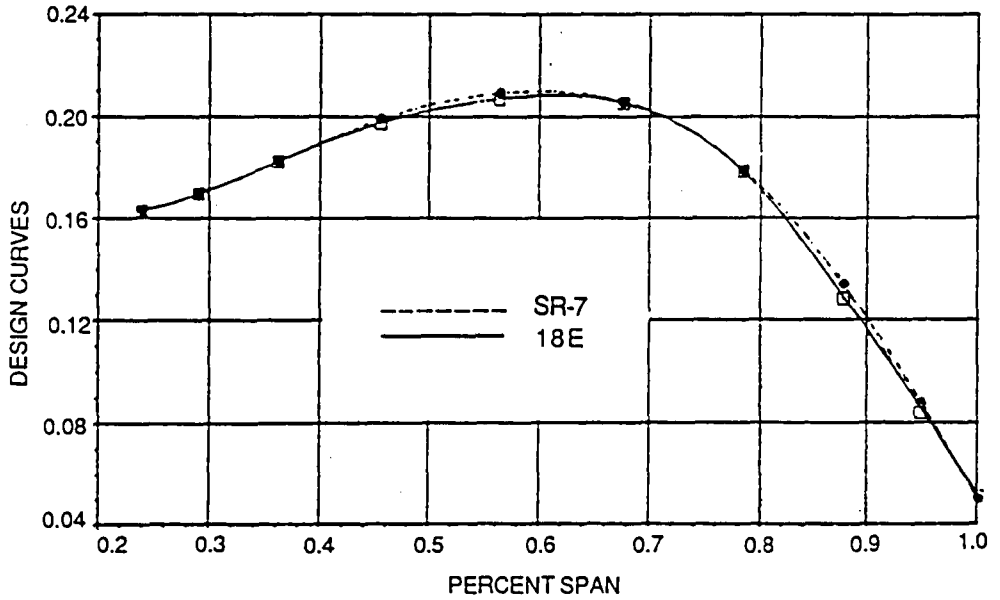

Figure 18. Design curve comparison overlays of the 18E and SR-7 designs - chord/diameter distribution.

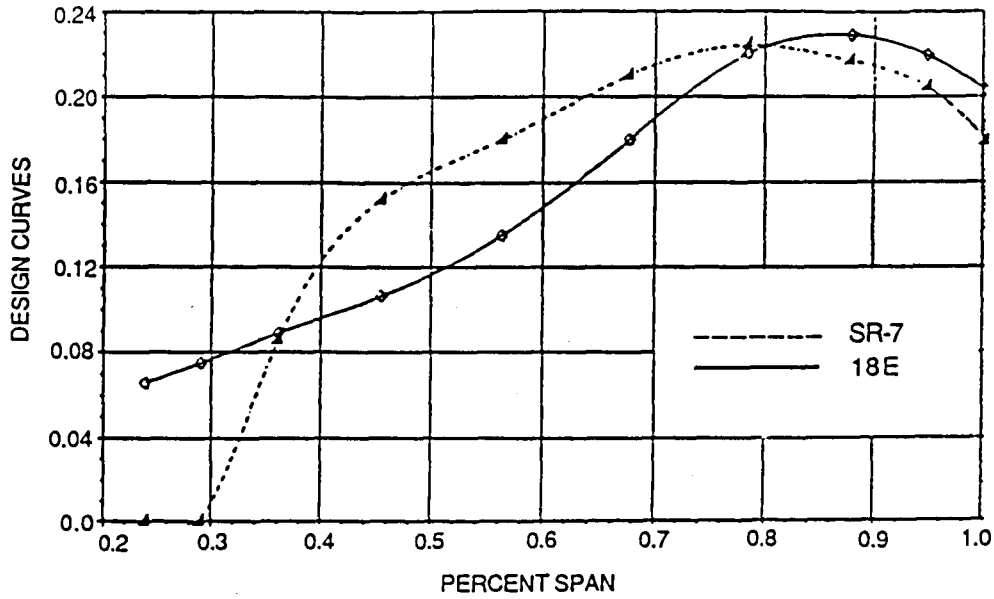

Figure 19. Design curve comparison overlays of the 18E and SR-7 designs - camber/lift coefficient distribution.

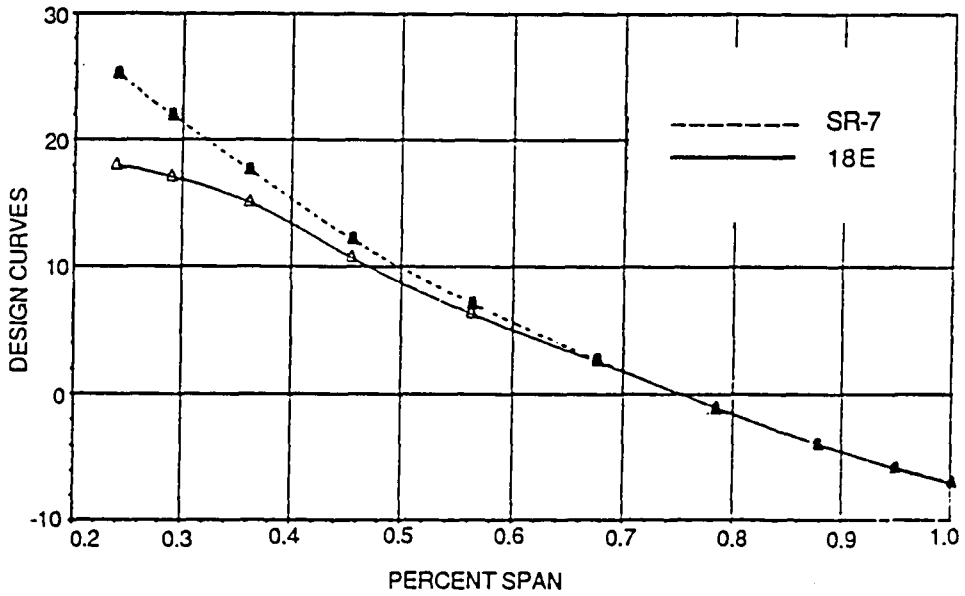

Figure 20. Design curve comparison overlays of the 18E and SR-7 designs - blade twist distribution.

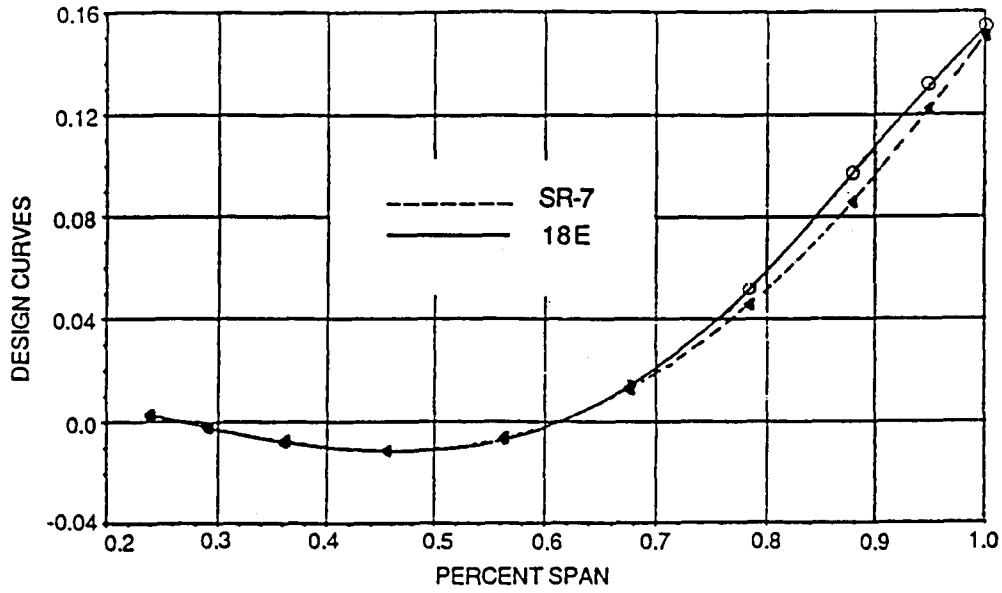

Figure 21. Design curve comparison overlays of the 18E and SR-7 designs - tangential stacking distribution.

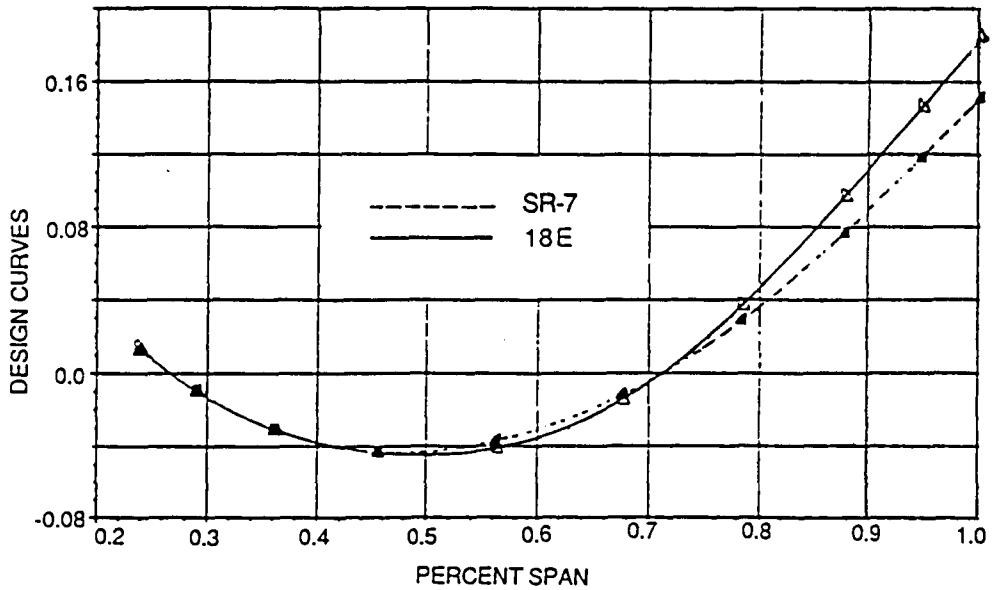

Figure 22. Design curve comparison overlays of the 18E and SR-7 designs - axial stacking distribution.

TABLE IX. THE SR-7 STAT OPTIMIZATION RESULTS

Large Variable Test Case

Design Variables	Prescribed Delta Limits from Initial Values	Delta Achieved
Exterior Geometry		
thickness/chord:		
25% span	-0.10 to 0.20	0.04677
43.75% span	-0.04 to 0.20	-0.00183
62.5% span	-0.02 to 0.20	-0.00088
81.25% span	-0.015 to 0.20	0.00072
100.% span	-0.005 to 0.20	-0.00500
chord:		
25% span	-16.2 to 2700 inches	0.93668
62.5% span	-16.2 to 2700 inches	0.03616
100.% span	-4.32 to 2700 inches	0.57302
lift coefficient:		
45.47% span	-0.15 to 1.0	-0.04704
78.45% span	-0.15 to 1.0	0.08776
100.% span	-0.15 to 1.0	0.28535
twist:		
45.47% span	-90. to 90. degrees	-0.01644
67.62% span	-90. to 90. degrees	-0.29220
78.45% span	-90. to 90. degrees	0.14895
100.% span	-90. to 90. degrees	-0.62752
tangential tilt:		
45.47% span	-1.E+5 to 1.E+5 inches	0.01603
67.62% span	-1.E+5 to 1.E+5 inches	0.06273
87.80% span	-1.E+5 to 1.E+5 inches	-0.03222
100.% span	-1.E+5 to 1.E+5 inches	0.93204
axial tilt:		
45.47% span	-1.E+5 to 1.E+5 inches	-0.10362
67.62% span	-1.E+5 to 1.E+5 inches	0.21488
87.80% span	-1.E+5 to 1.E+5 inches	-0.46021
100.% span	-1.E+5 to 1.E+5 inches	0.37737
Interior Geometry		
aluminum spar		
spar meanline:		
25.% span	-40. to 40.% chord	0.22064
62.5% span	-40. to 40.% chord	0.62621
100.% span	-40. to 40.% chord	0.63647
spar width:		
25.% span	-25. to 25.% chord	0.83816
62.5% span	-25. to 25.% chord	1.16400
100.% span	-25. to 25.% chord	0.04701
fiberglass shell		
shell thickness:		
25.% span	-0.03 to 1.0 inch	0.00378
62.5% span	-0.03 to 1.0 inch	0.00225
100.% span	-0.03 to 1.0 inch	-0.01143

TABLE IX. THE SR-7 STAT OPTIMIZATION RESULTS

Large Variable Test Case (continued)

Design Variables	Prescribed Delta Limits from Initial Values		Delta Achieved
EInterior Geometry			
nickel sheath			
sheath width:			
50.% span	-4.5 to 50.% chord		0.00000
75.% span	-12.5 to 50.% chord		-1.89890
100.% span	-22.5 to 50.% chord		11.20300
sheath thickness:			
50.% span	-0.019 to 1.0 inch		-0.00175
75.% span	-0.019 to 1.0 inch		0.00058
100.% span	-0.019 to 1.0 inch		0.00749
sheath cutoff:	-50 to 50% span		-0.45328
Design Constraints	**Limits**	**Initial**	**Final**
Resonances			
1st mode 2E	0.10 margin	-0.16745***	-0.19021
2nd mode 4E	0.05 margin	-0.30118	-0.30302
2nd mode 5E	0.025 margin	-0.44095	-0.44241
3rd mode 5E	0.025 margin	-0.17329	-0.13726
Steady Stress (Tsai-Wu)			
sheath	<1.0	0.04634	0.11491
shell	<1.0	0.05095	0.05106
foam	<1.0	0.00730	0.00282
spar	<1.0	0.00252	0.01029
One-P Force Response			
Life Fraction	<1.0	0.45857	1.13282 **
Flutter			
Flutter Mach Number	>1.0	1.0332	1.0545
Stall Flutter	>1.0	1.7509	1.7316
Driving Power	2592.	2592.	2582.2 *
Objective Function	**Initial**	**Final**	
DOC:			
efficiency	0.00004	-2.96046	
noise	-0.09135	-2.02210	
weight	-0.03293	-0.03627	
acquisition	-0.01490	-0.01348	
maintenance	-0.00546	-0.00494	
total =	-0.14460	-5.03716	
Efficiency - (%)	80.528	84.529	
Noise - (db)	143.43	139.73	
Weight - (lb)	42.170	43.144	

* active constraint
** violated constraint
*** minus sign indicates a satisfied frequency margin constraint

TABLE X. THE SR-7 STAT OPTIMIZATION RESULTS - BLADE RESTACK TO SOLVE VIOLATED STRESS CONSTRAINT

Design Variables	Initial Delta	Final Delta
Exterior Geometry		
twist:	...degrees	
45.47% span	-0.01644	-0.01645
67.62% span	-0.29220	-0.29220
78.45% span	0.14895	0.14898
100.% span	-0.62752	-0.62752
tangential tilt:	...inches	
45.47% span	0.01603	-0.11452
67.62% span	0.06273	-0.01893
87.80% span	-0.03222	-0.34029
100.% span	0.93204	0.98172
axial tilt:	...inches	
45.47% span	-0.10362	-0.19449
67.62% span	0.21488	0.21457
87.80% span	-0.46021	-0.66312
100.% span	0.37737	0.56592

Design Constraints	Limits	Initial	Final
Resonances			
1st mode 2E	0.10 margin	-0.19021	-0.19091
2nd mode 4E	0.05 margin	-0.30302	-0.30279
2nd mode 5E	0.025 margin	-0.44241	-0.44223
3rd mode 5E	0.025 margin	-0.13726	-0.13636
Steady Stress (Tsai-Wu)			
sheath	1.0	0.11491	0.08918
shell	1.0	0.05106	0.04861
foam	1.0	0.00282	0.00295
spar	1.0	0.01029	0.00950
One-P Force Response			
Life Fraction	1.0	1.13282 **	0.87552
Flutter			
Flutter Mach Number	1.0	1.0545	1.0882
Stall Flutter	1.0	1.7316	1.7284
Driving Power	2592.	2582.2 *	2566.3 *

Objective Function	Initial	Final
DOC:		
efficiency	-2.96046	-2.91146
noise	-2.02210	-2.53920
weight	-0.03627	-0.02423
acquisition	-0.01348	-0.01114
maintenance	-0.00494	-0.00408
total =	-5.03716	-5.49406
Efficiency - (%)	84.529	84.468
Noise - (db)	139.73	138.37
Weight - (lb)	43.144	43.189

* active constraint
** violated constraint

TABLE XI. REFINED VERSUS APPROXIMATE ANALYSES FOR THE INITIAL AND OPTIMUM SR-7 DESIGNS

	Hamilton Standard Refined	STAT Approximate	STAT Refined
Efficiency:			
initial...	79.4%	80.5%	80.1%
optimum...		84.5%	84.6%
Near-Field Noise:			
initial...	143 db	143.4 db	145.4 db
optimum...		138.4 db	146.0 db
Blade Weight:			
initial...	41.65 lbs	42.18 lbs	40.45 lbs
optimum...		43.19 lbs	41.31 lbs
Flutter:			
initial...	0.95 Mach	1.033 Mach	0.867 Mach
optimum...		1.088 Mach	0.911 Mach
Stall Flutter:			
initial...		1.751	1.760
optimum...		1.728	1.694
Driving Power:			
initial...		2592 hp	2526 hp
optimum...		2567 hp	2506 hp
Maximum Stress:			
initial...		11.0 kpsi	10.6 kpsi
optimum...		12.0 kpsi	12.1 kpsi
Blade Resonances:			
initial...			
1st mode		46.6 hz	46.8 hz
2nd mode		78.3 hz	78.0 hz
3rd mode		115.7 hz	114.1 hz
optimum...			
1st mode		45.3 hz	45.6 hz
2nd mode		78.1 hz	77.5 hz
3rd mode		120.9 hz	120.4 hz
Blade DOC:			
optimum...		-5.6%	-3.0%

8.3 THE AEROELASTIC SCALE MODEL - THE SR-7a

The SR-7a blade is an aeroelastic scale model representation of the SR-7 LAP blade design. The composite aeroelastic scale model (2/9 size) has a total of 12 separate layers. The blade shell is a uniform outer coat of 0.002 inch fiberglass and 3 layers of graphite intertwined among 4 layers of fiberglass cloth. The innermost fiberglass layer is glued to a titanium spar and the remaining gaps are filled with foam. The spar ends at 80.6 percent span, above which the blade is filled with fiberglass (fig. 23).

The exterior geometry of the blade is fixed to that of the SR-7 design, and therefore design variables are limited to alterations to the internal construction and the retention stiffness. The design constraints are all weighted into the objective function, since the final optimum will be a model with the identical static and dynamic characteristics of the SR-7 design which satisfies all design constraints.

STAT, using the current SR-7a geometry as an initial guess to the optimizer, improved the model dramatically in just 5 complete design moves which involved a total of 213 function calls, using 84 minutes of IBM 3090 computer time. The optimizer had not yet converged to an optimum design (i.e., it was allowed to make only 5 complete design moves) which implies that even greater improvements to the model could have been achieved. The results of this test case show that the objective function definition, as previously described, was adequately structured to properly account for aeroelastic differences between the full-scaled blade and its model. The results of the SR-7a STAT test case, including a comparison between the SR-7 and SR-7a aeroelastic properties, are summarized in Table XII and figure 24.

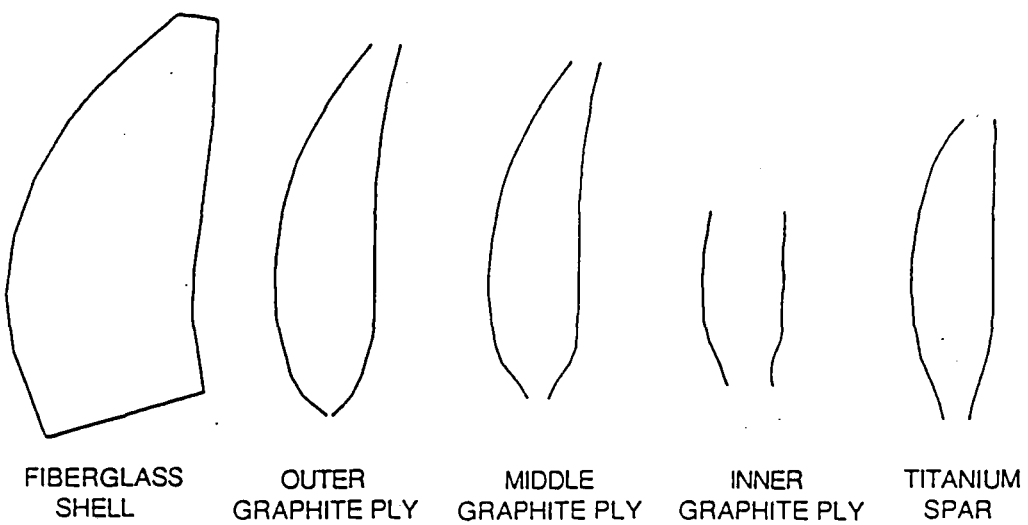

Figure 23. Composite construction of the SR-7a.

TABLE XII. THE SR-7a STAT OPTIMIZATION RESULTS

Design Variables	Delta Limits from Initial Values	Delta Achieved
Attachment		
Diameter	-1.0 to 2.0 inches	-0.05575
Length	-1.0 to 2.0 inches	-0.06378
Outer Graphite Ply		
lower cutoff	-100. to 100% span	0.28229
upper cutoff	-100. to 100% span	4.20610
ply orientation	-90. to 90. degrees	1.26720
ply meanline:		
30.% span	-25. to 25.% chord	0.72419
60.% span	-25. to 25.% chord	16.47200
90.% span	-25. to 25.% chord	7.09530
ply width:		
30.% span	-25. to 25.% chord	0.22693
60.% span	-25. to 25.% chord	10.22300
90.% span	-25. to 25.% chord	4.24170
Middle Graphite Ply		
lower cutoff	-100. to 100% span	-5.32560
upper cutoff	-100. to 100% span	5.05070
ply orientation	-90. to 90. degrees	-1.00770
ply meanline:		
35.% span	-25. to 25.% chord	2.17050
60.% span	-25. to 25.% chord	1.04900
85.% span	-25. to 25.% chord	1.79730
ply width:		
35.% span	-25. to 25.% chord	-0.13600
60.% span	-25. to 25.% chord	2.46400
85.% span	-25. to 25.% chord	2.60010
Inner Graphite Ply		
lower cutoff	-100. to 100% span	-4.82330
upper cutoff	-100. to 100% span	-0.71739
ply orientation	-90. to 90. degrees	0.30925
ply meanline:		
35.% span	-25. to 25.% chord	1.23910
47.5% span	-25. to 25.% chord	3.07600
60.% span	-25. to 25.% chord	0.39277
ply width:		
35.% span	-25. to 25.% chord	0.21038
47.5% span	-25. to 25.% chord	2.36390
60.% span	-25. to 25.% chord	-0.03735

TABLE XII. THE SR-7a STAT OPTIMIZATION RESULTS (continued)

Design Variables	Delta Limits from Initial Values	Delta Achieved
Titanium Spar		
upper cutoff	-100. to 100.% span	1.89600
spar meanline:		
25.% span	-25. to 25.% chord	-4.02210
50.% span	-25. to 25.% chord	24.42800
75.% span	-25. to 25.% chord	-5.91010
spar width:		
25.% span	-25. to 25.% chord	-2.09210
50.% span	-25. to 25.% chord	6.26880
75.% span	-25. to 25.% chord	1.77210
Fiberglass Filler		
lower cutoff	-100. to 100.% span	-1.68310

Objective Function	Initial	Final
mass distribution	0.44986	0.41948
resonances	0.02914	0.00620
static deflection	0.03898	0.13837
modal deflection	1.22790	0.62513
total value =	1.7485	1.1892

SR-7, SR-7a Comparison	SR-7	SR-7a Initial	SR-7a Final
Efficiency - (%)	81.589	82.695	81.644
Noise - (db)	143.44	143.24	143.47
Weight - (lb)	42.170	0.52737	0.45596
times scale factor cubed:		45.174	39.057
Driving Power - (hp)	2592.0	2453.4	2593.4
Flutter Mach Number	1.0332	1.0733	1.0051
Stall Flutter	1.7509	1.5782	1.6375
Resonances			
1st mode	46.623	218.59	206.12
divided by scale factor:		49.588	46.759
2nd mode	78.267	399.44	372.09
divided by scale factor:		90.614	84.409
3rd mode	115.74	502.78	507.19
divided by scale factor:		114.06	115.06

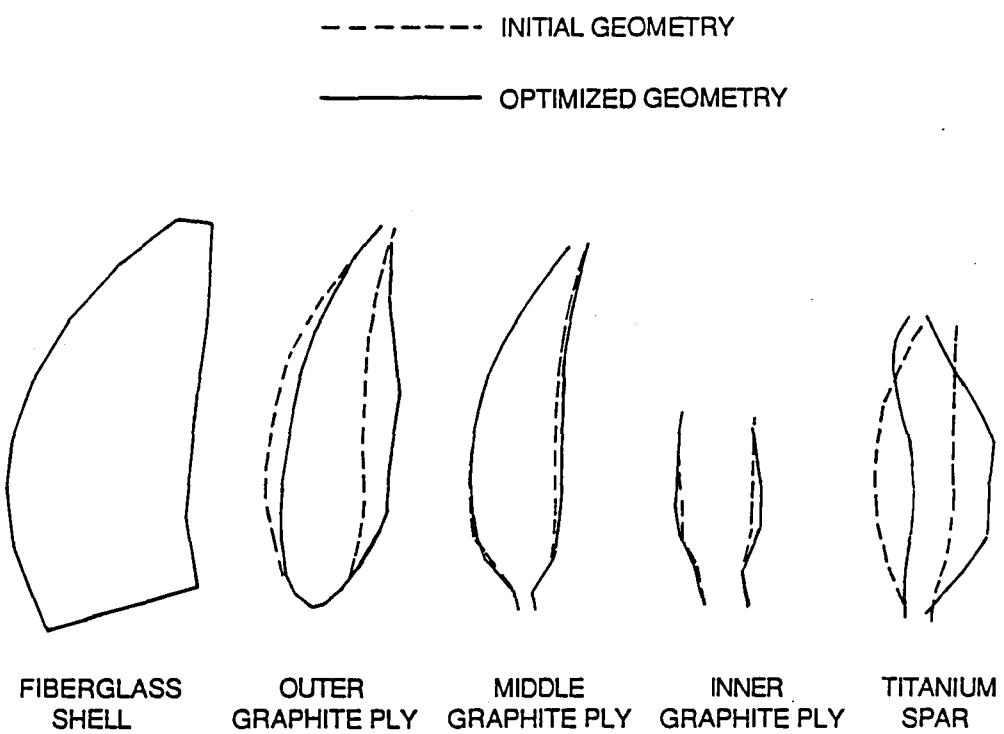

Figure 24. Initial and optimum design composite construction overlay plots of the SR-7a.

SECTION 9.0

CONCLUSIONS AND RECOMMENDATIONS

The STAT propfan optimization system has shown that design tailoring can effectively be applied to large, multi-disciplinary systems. The benefits of the system are evidenced by the difficult, lengthy development of the SR-7 Prop-Fan, which required 100 iterations through a manual design process to converge upon an acceptable, suboptimal design. As demonstrated by the Prop-Fan 18-E test case, the STAT system is able to coordinate the interdisciplinary requirements of propfan optimization, resolve unsatisfied constraints, and effectively improve a propfan design. In the case of the 18-E blade, STAT took an early design and improved upon it, locating a feasible blade that is superior to the SR-7 blade, which resulted from the tedious manual design process. The fact that STAT was able to achieve this design in one hour of IBM 3080 computer time is further evidence of the payoff from automating the propfan design process.

The successful improvement of the SR-7a scale model blade shows another potentially fruitful area for application of the optimization system. The flexibility allowed by the weighted differences objective function employed for this test case provides the capability to tune scale models for desired features, while maintaining acceptability of several other parameters. This capability can prove valuable for improving relevance of scale model wind tunnel testing.

The comparisons of the results of approximate optimization with refined analysis have revealed several deficiencies in the current STAT system, particularly with regard to the approximate acoustic analysis. The approximate acoustic analysis uses a tabular lookup and extrapolation procedure. Evidently, the current data base for the procedure is too limited in scope to cover the variety of designs that STAT desires to investigate, resulting in poor acoustic emissions estimates for designs that depart significantly from the original configurations. This problem can easily be resolved by adding data to the acoustic data base as refined results are produced for various blade configurations.

Recent studies have shown that counter rotation turboprops have the capability of fuel savings of up to an additional 10 percent over a single rotor propfan configuration. To include this configuration in the STAT system, the aerodynamic and efficiency analyses must be enhanced to include counter rotation effects. This enhancement is presently underway.

SECTION 10.0

REFERENCES

1. Vanderplaats, G. N., H. Sugimoto and C. M. Sprague, "ADS-1: A New General Purpose Optimization Program," AIAA 24th Structures, Structural Dynamics and Materials Conference, Lake Tahoe, Nevada, May, 1983.

2. Egolf, T. A., O. L. Anderson, D. E. Edwards and A. J. Landgrebe, "An Analysis for High Speed Propeller-Nacelle Aerodynamic Performance Prediction," Volumes I and II, United Technologies Research Center, R79-912949-19, June, 1979.

3. Borst H. V., "Summary of Propeller Design Procedures and Data," USAAMRDL TR 73-34A, November, 1973.

4. MacNeal, R. H., "The NASTRAN Theoretical Manual," NASA Sp-221 (01), April, 1972.

5. Jones, R. M., Mechanics of Composite Materials, Scripta Book Co., Washington, D. C., 1975.

6. Tsai, S. W. and E. M. Wu, "A General Theory of Strength for Anisotropic Materials," J. Composite Materials, Vol. 5, January, 1971, pp. 58-80.

7. Barmby, J. G., H. J. Cunningham and I. E. Garrick, "Study of Effects of Sweep on the Flutter of Cantilever Wings," NACA TN 2121, June, 1950.

8. Goldstein, S., "On the Vortex Theory of Screw Propellers," Royal Society (London) Proceedings, Vol. 123, No. 792, April 6, 1929.

9. Sullivan, W. E., J. E. Turnberg and J. A. Violette, "Large-Scale Advanced Prop-Fan SR-7 Blade," NASA Contract NAS3-23051, to be published.

DISTRIBUTION LIST

NASA-Lewis Research Center
Attn: Contracting Officer, MS 500-313
21000 Brookpark Road
Cleveland, OH 44135

NASA-Lewis Research Center
Attn: Tech. Report Control Office, MS 60-1
21000 Brookpark Road
Cleveland, OH 44135

NASA-Lewis Research Center
Attn: Tech. Utilization Office, MS 7-3
21000 Brookpark Road
Cleveland, OH 44135

NASA-Lewis Research Center
Attn: Division Contract File, MS 49-6
21000 Brookpark Road
Cleveland, OH 44135 (2 copies)

NASA-Lewis Research Center
Attn: Library, MS 60-3
21000 Brookpark Road
Cleveland, OH 44135

NASA-Lewis Research Center
Attn: D. A. Hopkins, MS 49-8
21000 Brookpark Road
Cleveland, OH 44135 (2 copies)

NASA-Lewis Research Center
Attn: C. C. Chamis, MS 49-8
21000 Brookpark Road
Cleveland, OH 44135

NASA-Lewis Research Center
Attn: L. Berke, MS 49-6
21000 Brookpark Road
Cleveland, OH 44135

NASA-Lewis Research Center
Attn: D. J. Gaunter, MS 49-8
21000 Brookpark Road
Cleveland, OH 44135

NASA-Lewis Research Center
Attn: R. H. Johns, MS 49-8
21000 Brookpark Road
Cleveland, OH 44135

NASA-Lewis Research Center
Attn: L. J. Kiraly, MS 23-3
21000 Brookpark Road
Cleveland, OH 44135

NASA-Lewis Research Center
Attn: J. A. Ziemianski, MS 86-1
21000 Brookpark Road
Cleveland, OH 44135

NASA-Lewis Research Center
Attn: P. B. Burstadt, MS 100-5
21000 Brookpark Road
Cleveland, OH 44135

NASA-Lewis Research Center
Attn: K. R. Kaza, MS 23-3
21000 Brookpark Road
Cleveland, OH 44135

NASA-Lewis Research Center
Attn: R. E. Kielb, MS 23-3
21000 Brookpark Road
Cleveland, OH 44135

NASA-Lewis Research Center
Attn: J. J. Adamczyk, MS 5-9
21000 Brookpark Road
Cleveland, OH 44135

DISTRIBUTION LIST (continued)

NASA-Lewis Research Center
Attn: R. D. Hager, MS 86-7
21000 Brookpark Road
Cleveland, OH 44135

NASA-Lewis Research Center
Attn: L. J. Bober, MS 86-7
21000 Brookpark Road
Cleveland, OH 44135

NASA-Lewis Research Center
Attn: G. K. Sievers, MS 86-7
21000 Brookpark Road
Cleveland, OH 44135

NASA-Lewis Research Center
Attn: J. F. Lubomski, MS 86-7
21000 Brookpark Road
Cleveland, OH 44135

National Aeronautics &
Space Administration
Attn: NHS-22/Library
Washington, DC 20546

National Aeronautics &
Space Administration
Attn: R/S. L. Venneri
Washington, DC 20546

National Aeronautics &
Space Administration
Attn: R/M. S. Hirschbein
Washington, DC 20546

NASA S&T Information Facility
Attn: Acquisition Department
P. O. Box 8757
Balt.-Wash. Int'l Airport, MD 21240

NASA Ames Research Center
Attn: Library, MS 202-3
Moffett Field, CA 94035

NASA John F. Kennedy Space Center
Attn: Library, MS AD-CSO-1
Kennedy Space Center, FL 32931

NASA Langley Research Center
Attn: Library, MS 185
Hampton, VA 23665-5225

NASA Langley Research Center
Attn: M. F. Card, MS 244
Hampton, VA 23665-5225

NASA Langley Research Center
Attn: W. J. Stroud, MS 191
Hampton, VA 23665-5225

NASA Goddard Space Flight Center
Attn: 252/Library
Greenbelt, MD 20771

NASA Lyndon B. Johnson Space Center
Attn: JM6/Library
Houston, TX 77001

NASA George C. Marshall Space
Flight Center
Attn: AS61/Library
Marshall Space Flt Center, AL 35812

DISTRIBUTION LIST (continued)

NASA George C. Marshall Space
Flight Center
Attn: R. S. Ryan
Marshall Space Flt Center, AL 35812

NASA George C. Marshall Space
Flight Center
Attn: L. Kieflin
Marshall Space Flt Center, AL 35812

Jet Propulsion Laboratory
Attn: Library
4800 Oak Grove Drive
Pasadena, CA 91103

Jet Propulsion Laboratory
Attn: B. Wada
4800 Oak Grove Drive
Pasadena, CA 91103

AFFDL/FBE
Attn: D. W. Smith
Wright-Patterson AFB, OH 45433

Air Force Aeronautical Prop. Lab.
Attn: I. Gershon
Wright-Patterson AFB, OH 45433

Air Force Aeronautical Prop. Lab.
Attn: N. Khot
Wright-Patterson AFB, OH 45433

Air Force Systems Command
Aeronautical Systems Division
Attn: Library
Wright-Patterson AFB, OH 45433

Air Force Systems Command
Aeronautical Systems Division
Attn: G. P. Sendeckyj
Wright-Patterson AFB, OH 45433

Air Force Office of Scientific
Research
Attn: A. K. Amos
Washington, DC 20333

Department of the Army
Attn: AMCRD-RC
U. S. Army Material Command
Washington, DC 20315

U.S. Army Ballistics Research Lab.
Attn: Dr. Donald F. Haskell, DRXBR-BM
Aberdeen Proving Ground, MD 21005

Army Mat'ls & Mech. Research Center
Attn: Dr. Donald W. Oplinger
Mechanics Research Laboratory
Watertown, MA 02172

U.S. Army Missile Command
Attn: Document Section
Redstone Scientific Info. Center
Redstone Arsenal, AL 35808

Commanding Officer
U.S. Army Research Office (Durham)
Attn: Library
Box CM, Duke Station
Durham, NC 27706

Bureau of Naval Weapons
Attn: RRRE-6
Department of the Navy
Washington, DC 20360

Commander
U.S. Naval Ordnance Laboratory
Attn: Library
White Oak
Silver Springs, MD 20910

Director, Code 6180
U.S. Naval Research Laboratory
Attn: Library
Washington, DC 20390

DISTRIBUTION LIST (continued)

Naval Air Propulsion Test Center
Attn: Mr. James Salvino
Aeronautical Engine Department
Trenton, NJ 08628

Naval Air Propulsion Test Center
Attn: Mr. Robert DeLucia
Aeronautical Engine Department
Trenton, NJ 08628

ARD-520
2100 Second Street, SW
Washington, DC 20591

Federal Aviation Administration DOT
Office of Aviation Safety, FOB 10A
Attn: Mr. John H. Enders
800 Independence Ave., SW
Washington, DC 20591

Federal Aviation Administration
Code ANE-214, Propulsion Section
Attn: Mr. Robert Berman
12 New England Executive Park
Burlington, MA 01803

National Bureau of Standards
Attn: R. Mitchell
Engineering Mechanics Section
Washington, DC 20234

National Transportation Safety Board
Attn: Mr. Edward P. Wizniak, MS TE-20
800 Independence Ave., SW
Washington, DC 20594

Aeronautical Research Association
of Princeton, Inc.
Attn: Dr. Thomas McDonough
P. O. Box 2229
Princeton, NJ 08540

Aerospace Corporation
Attn: Library-Documents
2400 E. El Segundo Blvd.
Los Angeles, CA 90045

Allison Gas Turbine Operation
General Motors Corporation
Attn: Mr. William Springer
Speed Code T3, Box 894
Indianapolis, IN 46206

AVCO Lycoming Division
Attn: Mr. Herbert Kaehler
550 South Main Street
Stratford, CT 06497

Beech Aircraft Corporation
Attn: Mr. M. K. O'Connor
Wichita, KA 67201

Bell Aerospace
Attn: R. A. Gellatly
P. O. Box 1
Buffalo, NY 14240

Boeing Aerospace Company
Impact Mechanics Lab
Attn: Dr. R. J. Bristow
P. O. Box 3999
Seattle, WA 98124

Boeing Commercial Airplane Company
Attn: Dr. Ralph B. McCormick
P. O. Box 3707
Seattle, WA 98124

Boeing Commercial Airplane Company
Attn: Mr. David T. Powell, MS 73-01
P. O. Box 3707
Seattle, WA 98124

Boeing Commercial Airplane Company
Attn: Dr. John H. Gerstle
P. O. Box 3707
Seattle, WA 98124

DISTRIBUTION LIST (continued)

Boeing Company
Attn: Library
Wichita, KA 67201

Douglas Aircraft Company
Attn: M. A. O'Connor, Jr., MS 36-41
3855 Lakewood Blvd.
Long Beach, CA 90846

Garrett AiResearch Manufacturing Co.
Attn: L. A. Matsch
111 S. 34th Street
P. O. Box 5217
Phoenix, AZ 85010

Garrett Turbine Engine Company
Mechanical Component Design
111 S. 34th Street
P. O. Box 5217
Phoenix, AZ 85010

General Dynamics
Attn: Library
P. O. Box 748
Fort Worth, TX 76101

General Dynamics/Convair Aerospace
Attn: Library
P. O. Box 1128
San Diego, CA 92112

General Electric Company
Attn: Dr. L. Beitch, MS K221
Interstate 75, Bldg. 500
Cincinnati, OH 45215

General Electric Company
Attn: Dr. R. L. McKnight, MS K221
Interstate 75, Bldg. 500
Cincinnati, OH 45215

General Electric Company
Attn: Dr. V. Gallardo, MS K221
Interstate 75, Bldg. 500
Cincinnati, OH 45215

General Electric Company
Aircraft Engine Group
Attn: Mr. Herbert Garten
Lynn, MA 01902

Grumman Aircraft Engineering Corp.
Attn: Library
Bethpage, Long Island, NY 11714

Grumman Aircraft Engineering Corp.
Attn: H. A. Armen
Bethpage, Long Island, NY 11714

Lawrence Livermore Laboratory
Attn: Library
P. O. Box 808, L-42
Livermore, CA 94550

Lockheed Palo Alto Research Labs
Attn: Dr. D. Bushnell
Palo Alto, CA 94304

Lockheed Missiles and Space Company
Huntsville Research & Eng'rg Center
Attn: H. B. Shirley
P. O. Box 1103
Huntsville, AL 18908

Lockheed California Company
P. O. Box 55
Dept. 75-71, Pl. A-1
Burbank, CA 91520

MacNeal-Schwendler Corporation
Attn: R. H. MacNeal
7442 North Figueroa Street
Los Angeles, CA 90041

DISTRIBUTION LIST (continued)

MARC Analysis Research Corporation
Attn: J. Nagtegaal
260 Sheriden Avenue, Suite 314
Palo Alto, CA 94306

McDonnell Douglas Aircraft Corp.
Attn: Library
P. O. Box 516
Lambert Field, MO 63166

Mechanical Technologies, Inc.
Attn: M. S. Darlow
Latham, NY 12110

Northrop Space Laboratories
Attn: Library
3401 West Broadway
Hawthorne, CA 90250

North American Rockwell, Inc.
Rocketdyne Division
Attn: Library, Dept. 596-306
6633 Canoga Avenue
Canoga Park, CA 91304

North American Rockwell, Inc.
Rocketdyne Division
Attn: J. F. Newell
6633 Canoga Avenue
Canoga Park, CA 91304

North American Rockwell, Inc.
Space & Information Systems Div.
Attn: Library
12214 Lakewood Blvd.
Downey, CA 90241

Norton Company
Attn: Mr. George E. Buron
Industrial Ceramics Div.
Armore & Spectramic Products
Worcester, MA 01606

Norton Company
Industrial Ceramics Division
Attn: Mr. Paul B. Gardner
1 New Bond Street
Worcester, MA 01606

Republic Aviation
Fairchild Hiller Corporation
Attn: Library
Farmingdale, NY 11735

Rockwell International Corporation
Attn: Joseph Gausselin-D422/402AB71
Los Angeles International Airport
Los Angeles, CA 90009

Rohr Industries
Attn: Mr. John Meaney
Foot of H Street
Chula Vista, CA 92010

Southwest Research Institute
Attn: Dr. T. A. Cruse
P. O. Box 28510
Culebra Road
San Antonio, TX 78284

TWA, Inc.
Attn: Mr. John J. Morelli
Kansas City International Airport
P. O. Box 20126
Kansas City, MO 64195

United Technologies Corporation
Pratt & Whitney
Attn: Library, MS 732-11
P. O. Box 109600
West Palm Beach, FL 33402

United Technologies Corporation
Pratt & Whitney
Attn: R. A. Marmol, MS 713-39
P. O. Box 109600
West Palm Beach, FL 33402

DISTRIBUTION LIST (continued)

United Technologies Corporation
Pratt & Whitney
Attn: Library, MS 169-31
400 Main Street
East Hartford, CT 06108

United Technologies Corporation
Pratt & Whitney
Attn: R. Liss, MS 162-30
400 Main Street
East Hartford, CT 06108

United Technologies Corporation
Pratt & Whitney
Attn: D. H. Hibner, MS 163-09
400 Main Street
East Hartford, CT 06108

United Technologies Corporation
Hamilton Standard
Attn: Dr. R. A. Cornell
Windsor Locks, CT 06096

United Technologies Corporation
Hamilton Standard
Attn: Dr. G. P. Towsend
Windsor Locks, CT 06096

United Technologies Research Center
Attn: Dr. A. Dennis, MS 18
Silver Lane
East Hartford, CT 06108

University of Akron
Attn: Dr. Paul Chang
Department of Civil Engineering
Akron, OH 44325

University of Arizona
Attn: H. Kamel
College of Engineering
Tucson, AZ 87521

University of California
Attn: E. Wilson
Department of Civil Engineering
Berkeley, CA 94720

University of California
Attn: L. A. Schmit, Jr.
Mechanics & Structures Department
School of Eng'rg & Applied Science
Los Angeles, CA 90024

Columbia University
Attn: R. Vaicaitis
New York, NY 10027

Columbia University
Attn: G. Desgupta
New York, NY 10027

University of Dayton Research Inst.
Attn: F. K. Bogner
Dayton, OH 45409

Georgia Institute of Technology
Attn: S. N. Atluri
School of Civil Engineering
Atlanta, GA 30332

Georgia Institute of Technology
Attn: G. J. Simitses
225 North Avenue
Atlanta, GA 30332

Univ. of Illinois at Chicago Circle
Department of Materials Engineering
Attn: Dr. Robert L. Spilker
Box 4348
Chicago, IL 60680

IIT Research Institute
Technology Center
Attn: Library
Chicago, IL 60616

DISTRIBUTION LIST (continued)

Lehigh University
Inst. of Fracture & Solid Mechanics
Attn: G. T. McAllister
Bethlehem, PA 18015

University of Kansas
Attn: R. H. Dodds
School of Engineering
Lawrence, KS 66045

Massachusetts Institute of Technology
Attn: K. Bathe
Cambridge, MA 02139

Massachusetts Inst. of Technology
Attn: T. H. Pian
Cambridge, MA 02139

Massachusetts Inst. of Technology
Attn: J. Mar
Cambridge, MA 02139

Massachusetts Inst. of Technology
Attn: E. A. Witmer
Cambridge, MA 02139

Massachusetts Inst. of Technology
Attn: J. Dugundji
Cambridge, MA 02139

State Univ. of New York at Buffalo
Attn: P. K. Banerjee
Department of Civil Engineering
Buffalo, NY 14225

Northwestern University
Attn: T. Belytschko
Department of Civil Engineering
Evanston, IL 60201

Ohio State University
Attn: Prof. N. Sarigul
Dept. of Aero. and Astro. Engrg.
2036 Neil Avenue Mall
Columbus, OH 43210-1276

Purdue University
Attn: C. T. Sun
School of Aeronautics & Astronautics
West Lafayette, IN 47907

Rensselaer Polytechnic Institute
Attn: R. Loewy
Troy, NY 12181

Stanford University
Attn: T. J. R. Hughes
School of Engineering
Stanford, CA 94305

Stevens Institute of Technology
Attn: F. Sisto
Castle Point Station
Hoboken, NJ 07030

Texas A&M University
Attn: W. E. Haisler
Aerospace Engineering Department
College Station, TX 77843

University of Texas at Austin
Attn: J. T. Oden
College of Engineering
Austin, TX 78712-1085

University of Virginia
Attn: E. J. Gunter
School of Eng'rg & Applied Science
Charlottesville, VA 22901

V.P.I. and State University
Attn: R. H. Heller
Department of Engineering Mechanics
Blacksburg, VA 24061

Worcester Polytechnic Institute
Attn: J. H. Kane
Computer Aided Engineering Center
Worcester, MA 01609

End of Document